BOUNDS ON CAUSAL PARAMETERS OF PROSPECTIVE GROUND MOTIONS AND THEIR EFFECT ON CHARACTERISTICS OF SELECTED GROUND MOTIONS

Karim Tarbali & Brendon A. Bradley

Research report 2015-01

Department of Civil and Natural Resources Engineering

University of Canterbury

New Zealand

January 2015

ISSN: 1172-9511

Abstract

In this study, the effect of considering bounds on causal parameters of prospective ground motions (e.g., magnitude, source-to-site distance, and site condition) for the purpose of ground-motion selection is investigated. Although using bounds on causal parameters is common practice in conventional approaches for ground motion selection, there is presently no consistent approach for setting these bounds as a function of the seismic hazard at the site. A rigorous basis is developed and sensitivity analyses performed for the consideration of bounds on magnitude, source-to-site distance, and site condition for use in ground motion selection. In order to empirically illustrate the effects of various causal parameter bounds on the characteristics of selected ground motions, 78 and 36 cases of scenario seismic hazard analysis (scenario SHA) and probabilistic seismic hazard analysis (PSHA) are considered, which cover a wide range of causal parameters and site conditions. Ground motions are selected based on the generalized conditional intensity measure (GCIM) approach, which considers multiple ground motion intensity measures (IMs) and their variability in order to appropriately represent characteristics of the seismic hazard at the site. It is demonstrated that the application of relatively 'wide' bounds on causal parameters effectively removes ground motions with drastically different characteristics with respect to the target seismic hazard (improving computational efficiency in the selection process by reducing the subset of prospective records), and results in an improved representation of the target causal parameters. In contrast, the use of excessively 'narrow' bounds can lead to ground motion ensembles with a poor representation of the target IM distributions, especially for ground motions selected to represent PSHA results. As a result, the causal parameter bound criteria advocated in this study provide a good 'default' that is expected to be sufficient in the majority of problems encountered in seismic hazard and demand analyses.

Table of Contents

List of Figures

List of Tables

1 Introduction

Selecting appropriate ground motion ensembles is a key step in assessing the seismic performance of engineered systems through dynamic seismic response analyses. Various methods have been proposed to select ground motions for seismic response analysis (e.g., McGuire 1995, Shome et al. 1998, Bommer and Acevedo 2004, Kottke and Rathje 2008, Baker 2010, Jayaram et al. 2011, Wang 2011, Bradley 2012c). Generally, ground motion selection is conducted based on implicit and explicit measures of ground motion intensity (Bommer and Acevedo 2004). Implicit measures of ground motion are parameters that do not directly characterize the severity of ground motions, such as magnitude, source-to-site distance, site condition, and are often referred to as (implicit) causal parameters. On the other hand, explicit intensity measures (IMs) such as spectral acceleration, peak ground velocity, duration, among others are directly related to the ground motion time series itself. It is common in ground motion selection practice to first constrain the database of prospective ground motions based on causal parameters similar to those of earthquakes dominating the seismic hazard for the site (Bommer and Acevedo 2004, Baker 2010, Wang 2011), and then select ground motions based on an explicit IM-based target, most commonly an acceleration spectrum from either site-specific seismic hazard analysis or general design guidelines (see Katsanos et al. 2010 and the references therein).

Despite the prevalent application of causal parameter bounds prior to the ground motion selection process (Katsanos et al. 2010), specifying the limits of the bounds is a subjective choice. For instance, Stewart et al. (2001) recommended that, because of the considerable effect of magnitude on characteristics of ground motions, ±0.25 magnitude (M_w) units either side of a considered scenario rupture is a desirable bound. Bommer and Acevedo (2004) recommended $\pm 0.2 M_w$ units from the scenario magnitude as the bound on prospective ground motions. In order to include an adequate number of ground motions when this M_w bound is applied, they comment that the source-to-site distance of records can be bounded over a wider range, without specifically mentioning a limit. In terms of site condition, both Stewart et al. (2001) and Bommer and Acevedo (2004) noted the importance of considering records from site conditions compatible with the site of interest. However, in cases where the application of bounds on magnitude and source-to-site distance restricts the number of available ground motions, Bommer and Acevedo (2004) recommended considering ground motions from sites with one site classification (based on NEHRP (2003) or CEN (2005)) either side of the in-situ site condition. Considering the tectonic regime of ground motions

(e.g., active shallow crustal or subduction-zone), style of faulting, selecting from multiple events and multiple recording stations within an event are also advocated (e.g., Bommer and Acevedo 2004, Wang et al. 2013). Literature discussing other common ground motion selection methods (e.g., Kottke and Rathje 2008, Baker 2010, Jayaram et al. 2011, Wang 2011) has also noted the application of causal parameter bounds, however, generally a quantitative approach by which such bounds can be applied is not provided. It is also important to note that the majority of literature commenting on the use of causal parameter bounds is cast in the context of a scenario earthquake of interest, and thus the specific bounds for use in ground motion selection based on PSHA (which is the summation of the hazard from numerous earthquake sources as quantified via deaggregation) is not obvious.

Historically, a primary reason for using causal parameter bounds in ground motion selection stems from the fact that considering spectral acceleration (SA) ordinates as the only explicit IM does not adequately account for an accurate representation of ground motion duration and cumulative effects (Bommer et al. 2004, Wang 2011, Bradley 2012c, Tarbali and Bradley 2014a, b). Ground motion selection should be principally based on explicit ground motion IMs, rather than implicit causal parameters which are not a direct representation of the ground motion at the site (Shome et al. 1998, Baker and Cornell 2006, Baker 2010, Bradley 2012c).

In contrast to the conventional use of causal parameter bounds to address the shortcomings of selecting ground motions based on only SA ordinates, ground motion selection based on the generalized conditional intensity measure (GCIM) approach (Bradley 2010a) utilizes multiple explicit IMs which can directly represent ground motion amplitude, frequency content, duration, and cumulative effects. As a result, GCIM-based ground motion selection without the need to consider causal parameter bounds has been demonstrated for both probabilistic and scenario seismic hazard analyses (Bradley 2012c, Tarbali and Bradley 2014b). However, even with the GCIM method (among others), causal parameter bounds can assist in removing those records that have drastically different characteristics compared to the target seismic hazard at the site. Moreover, the application of such bounds will improve the computational efficiency of the selection process by decreasing the size of empirical ground motion databases considered. The latter point is particularly pertinent when comparing the ever-increasing size of empirical databases, for example, comparing the NGA-West1 (Chiou et al. 2008) and NGA-West2 (Ancheta et al. 2013) databases reveals that the number of ground motion records has increased six-fold from 3,551 to 21,336, and the range of the

causal parameters of ground motions has also broadened (see Table 1). Despite this large increase in empirical database size, approximately half of the NGA-West2 database (i.e., 10,706 records) are from events with magnitude less than 4.5 (Bozorgnia et al. 2014), which are generally not of engineering interest for ground motion selection relating to seismic hazard analysis in regions with moderate-to-high seismicity.

Table 1: Comparison between the NGA-West1 and NGA-West2 empirical ground motion databases and causal parameter ranges

	Magnitude, M_w	source-to-site distance (R_{rup}, km)	Site condition (V_{s30}, m/sec)	Number of Events	Number of records
NGA-West1[*]	[4.2 , 7.9]	[0.2 , 300]	[116 , 2016]	173	3,551
NGA-West2[**]	[3.0 , 7.9]	[0.05 , 1533]	[94 , 2100]	600	21,336

[*] Chiou et al. (2008)

[**] Ancheta et al. (2013)

From the above discussion it can be seen that it is advantageous to utilize causal parameter bounds for preliminary 'screening' of empirical ground motion databases prior to the primary ground motion selection process based on explicit IMs. In this study, the consideration of bounds on magnitude, source-to-site distance, and site condition of prospective ground motions as a function of the seismic hazard at the site is rigorously examined. 78 scenario SHA and 36 PSHA cases are considered which encompass a broad range of rupture scenarios (including varying deaggregation distributions) and site conditions for ground motion selection. Ground motions are selected based on the GCIM methodology (Bradley 2010a), which has been developed for both PSHA- and scenario-based ground motion selection (Bradley 2012c, Tarbali and Bradley 2014b), and is a generalization of the conditional mean spectrum method (Baker and Cornell 2006, Baker 2010). The effect of causal parameter bound selection on both the number of available prospective ground motions from an initial empirical as-recorded database, and the statistical properties of IMs of selected ground motions using the GCIM-based approach are examined.

2 Ground-motion selection for scenario seismic hazard analysis (scenario SHA)

Scenario-based seismic performance assessment involves obtaining the seismic response of the system given the occurrence of a scenario earthquake with specified rupture characteristics. For system-specific dynamic analyses, such performance assessment requires

the selection of ground motion ensembles to represent characteristics of the predicted ground shaking at the site. Since there is a variability in the predicted ground motion intensity for a given scenario earthquake, selected ground motions should aim to explicitly represent this variability (Kottke and Rathje 2008, Bradley 2010a, Jayaram et al. 2011, Wang 2011, Bradley 2012c). In addition, since the severity of ground motions cannot be completely presented based on only spectral acceleration ordinates, multiple IMs accounting for amplitude, frequency content, duration, and cumulative effects should be considered to select ground motions with an appropriate representation for these different aspects (Bradley 2010a, 2012c).

The aforementioned issues to be considered in scenario-based ground motion selection are directly addressed in the GCIM-based ground motion selection methodology for scenario earthquakes presented by Tarbali and Bradley (2014b). In summary, the GCIM method uses the conditional multivariate distribution of a considered vector of IMs, $\boldsymbol{IM}$, as the target to assess the appropriateness of the ensemble of selected ground motions. A so-called weight vector is used to prescribe the relative importance of the considered IMs in the selection process and calculate the misfit of each prospective ground motion with respect to the target distribution (Bradley 2012c, Tarbali and Bradley 2014b). A global misfit is also used to quantify the difference between the selected ground motion ensemble and the target distribution (Bradley 2013), as defined by Equation (1):

$$R = \sum_{i=1}^{N_{IM}} w_i (D_{IM_i})^2 \quad \textbf{(1)}$$

where w_i is the weight vector value for the i^{th} intensity measure (i.e., IM_i); and D_{IM_i} is the Kolmogorov-Smirnov (KS) test statistic, which is the maximum difference between the empirical distribution (of the selected ground motions) and the corresponding target IM_i distribution. Thus, the global misfit, R, consists of the mismatch between the empirical and target distributions of all of the IMs in $\boldsymbol{IM}$, based on the relative importance defined by the weight vector. Herein, both the distribution of selected ground motions in comparison to the target distribution, and the global misfit, R, are used to compare the appropriateness of the ensembles selected with and without causal parameter bounds.

2.1 Rupture scenarios and site conditions considered

In order to empirically investigate the effects of causal parameter bounds on the characteristics of selected ground motions, 78 scenario ruptures are considered which encompass a wide range of implicit causal parameters for scenario earthquakes of interest in moderate-to-high seismicity regions. Table 2 summarizes the characteristics of the considered rupture scenarios and site conditions. As presented in Table 2, the considered rupture scenarios range from magnitude M_w=5.5-8.0 and source-to-site distance R_{rup}=5-120 km. Importantly, the maximum R_{rup} for each M_w is selected to ensure that only ground motion amplitudes of engineering importance are considered (e.g., only R_{rup}=5, 15 km is considered for M_w=5.5 scenarios). This is further illustrated in Figure 1, in which the median peak ground acceleration (PGA) of the considered rupture scenarios is presented. As shown, all the considered scenarios result in median PGAs above 0.05g for the example site condition.

Table 2: Characteristics of the 78 considered scenario ruptures and site conditions for scenario-based ground motion selection

Magnitude, M_w	Source-to-site distance, R_{rup} (km)	Site condition, V_{s30}(m/s)	Fault type
5.5	5, 15	200, 400, 800	Strike-slip
6.0	5, 15, 30	200, 400, 800	Strike-slip
6.5	5, 15, 30, 50	200, 400, 800	Strike-slip
7.0	5, 15, 30, 50, 80	200, 400, 800	Strike-slip
7.5	5, 15, 30, 50, 80, 120	200, 400, 800	Strike-slip
8.0	5, 15, 30, 50, 80, 120	200, 400, 800	Strike-slip

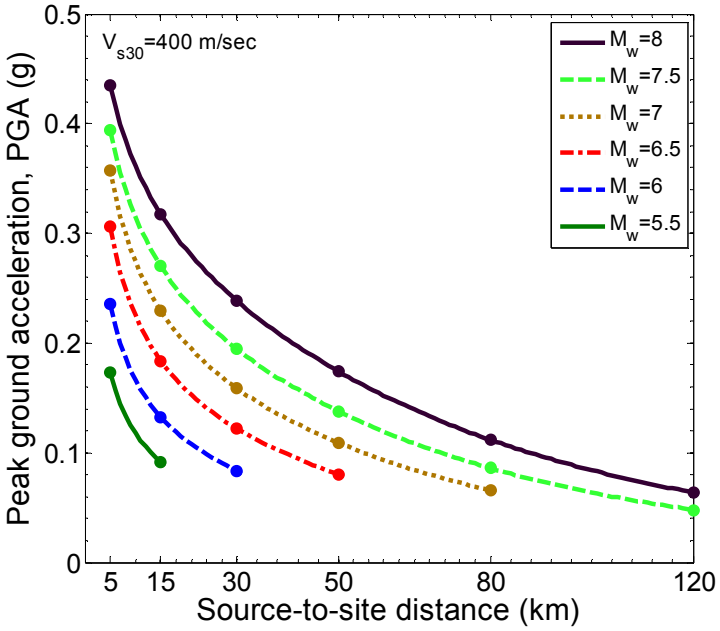

Figure 1: Median peak ground acceleration (PGA) for the considered scenario ruptures for V_{s30}=400 m/s site condition (points indicate the considered scenarios in Table 2) illustrating the magnitude-dependent R_{rup} limits in order to consider only significant ground motion amplitudes.

Three different site conditions, with a 30 m time-averaged shear wave velocity (i.e., V_{s30}) of 200, 400, and 800 m/s, are considered for each $M_w - R_{rup}$ combination. These V_{s30} values were chosen to represent typical soft soil, stiff soil, and soft rock conditions, approximately corresponding to NEHRP site classes D, C, and A/B, respectively (NEHRP 2003). Strike-slip faulting is chosen as the only rupture mechanism for the scenarios considered, as evidence suggests that focal mechanism tends to result in a relatively systematic variation in ground motion intensity, with little effect on frequency content or duration, and thus is adequately captured through simple amplitude scaling (Bommer et al. 2003). For this reason others have also advised that, relative to other variables, focal mechanism can be neglected as a causal parameter of importance when selecting ground motions (e.g., ASCE/SEI7-10 2010).

2.2 Bounds considered on implicit causal parameters

As previously mentioned, the aim of considering causal parameter bounds is to remove ground motions in empirical as-recorded databases that have drastically different characteristics with respect to the target rupture scenario. However, the remaining database should still be large enough to select the desired number of ground motions which can appropriately represent the multiple IM distributions of interest. It is important to reiterate

that the process of obtaining a ground motion ensemble which represents the target multivariate distribution of $\boldsymbol{IM}$ is based solely on the explicit ground motion IMs. Thus, causal parameter bounds are only a screening criteria applied prior to the ground motion selection process based on explicit IMs. In this regard, the bounds considered in this study are 'wide' in order to avoid excessive removal of potentially reasonable ground motions. Various sensitivity analyses are conducted to determine the bounds. As presented by Tarbali and Bradley (2014a), the application of bounds wider than those considered in this study leads to results consistent with those presented in this study. Also, the drawbacks of using narrower bounds, similar to those proposed by Stewart et al. (2001) and Bommer and Acevedo (2004) are discussed subsequently based on the number of available ground motions (presented in Table 5).

Table 3 presents the considered bounds for magnitude, source-to-site distance, and site condition of prospective ground motions for scenario-based ground motion selection. As shown, ground motions are bounded to half of a magnitude greater and smaller than the scenario magnitude. This is twice as large as the magnitude bound recommended by Stewart et al. (2001) and Bommer and Acevedo (2004). Also, the R_{rup} of prospective ground motions are bounded to 0.5 to 1.5 times the scenario R_{rup} (except 'near-fault' scenarios for which R_{rup} ≤15 km, where the R_{rup} bound is set to values less than 30 km). The site condition of prospective ground motions are also limited to 0.5 to 1.5 times the V_{s30} of the site, ensuring that ground motions within similar soil classes are included for each site condition. It is noted that the R_{rup} and V_{s30} bounds considered in this study are similar to those implicitly recommended by Stewart et al. (2001) and Bommer and Acevedo (2004).

Table 3: Bounds on the implicit causal parameters of prospective ground motions for scenario-based ground motion selection

Causal parameters	Lower limit	Upper limit
Magnitude, M_w=5.5, 6.0, 6.5, 7.0, 7.5, 8.0	$M_w - 0.5$	$M_w + 0.5$
Site condition, V_{s30}(m/s) =200, 400, 800	$0.5V_{s30}$	$1.5V_{s30}$
Source-to-site distance, R_{rup}(km)= $5, 15$	0 km	30 km
Source-to-site distance, R_{rup}(km)= $30, 50, 80, 120$	$0.5R_{rup}$	$1.5R_{rup}$

For each of the 78 scenarios in Table 2, it is beneficial to understand the number of ground motions that will be available for ground motion selection before and after the abovementioned bounds are applied. Table 4 presents the number of available records, N_{rec},

from the NGA-West1 database (Chiou et al. 2008) for the considered scenarios after application of the bounds presented in Table 3. It is noted that since the ground motion time series in the NGA-West2 database (Ancheta et al. 2013) were not available at the time of this study, the NGA-West1 was adopted as the prospective database unless otherwise noted. Based on the available information on various characteristics of the recorded ground motions, a total of 3222 ground motions from the NGA-West1 database are utilized here for each of the considered scenarios (before the application of causal parameter bounds). As shown in Table 4, the number of ground motions after the application of causal parameter bounds for the V_{s30}=400 m/s site condition (i.e., V_{s30} range from 200 to 600 m/s) is greater than that for the V_{s30}=200 and 600 m/s site conditions (i.e., V_{s30} range from 100 to 300 and 400 to 1200 m/s, respectively).

Table 4: Number of available ground motion records (N_{rec}) from the NGA-West1 database based on the applied bounds for scenario-based ground motion selection cases

Site condition V_{s30}=200 m/s

scenario	R_{rup}=5	R_{rup}=15	R_{rup}=30	R_{rup}=50	R_{rup}=80	R_{rup}=120
M_w=5.5	86	86	-	-	-	-
M_w=6.0	66	66	108	-	-	-
M_w=6.5	93	93	104	201	-	-
M_w=7.0	68	68	48	54	55	-
M_w=7.5	22	22	30	47	119	119
M_w=8.0	20	20	30	39	105	93

Site condition V_{s30}=400 m/s

scenario	R_{rup}=5	R_{rup}=15	R_{rup}=30	R_{rup}=50	R_{rup}=80	R_{rup}=120
M_w=5.5	292	292	-	-	-	-
M_w=6.0	268	268	409	-	-	-
M_w=6.5	234	234	349	667	-	-
M_w=7.0	145	145	143	195	210	0
M_w=7.5	97	97	77	173	285	280
M_w=8.0	76	76	59	126	211	152

Site condition V_{s30}=800 m/s

scenario	R_{rup}=5	R_{rup}=15	R_{rup}=30	R_{rup}=50	R_{rup}=80	R_{rup}=120
M_w=5.5	128	128	-	-	-	-
M_w=6.0	134	134	210	-	-	-
M_w=6.5	124	124	204	445	-	-
M_w=7.0	68	68	68	83	89	-
M_w=7.5	76	76	47	124	171	127
M_w=8.0	61	61	40	109	147	95

In order to compare the effect of using narrower causal parameter bounds on the number of available ground motions, the magnitude bound recommended in Bommer and Acevedo (2004), i.e., $\pm 0.2M_w$ units from the scenario magnitude, is used to obtain the number of available ground motions for the considered scenarios (while the R_{rup} and V_{s30} bounds are the same as used earlier). Table 5 presents the result of applying this narrow bound for all of the considered scenarios, which illustrates that the number of available ground motions is restrictively small for most of the considered rupture scenarios, with the average number of available motions being only 43% of those using the $\pm 0.5M_w$ bound. As illustrated later in Figure 4, ground motions selected based on such a small number of prospective motions may have a poor representation of the target IM distributions, because the narrow causal parameter bounds remove ground motions that can still appropriately represent the target scenario hazard.

Table 5: Number of available ground motion records (N_{rec}) from the NGA-West1 database based on the R_{rup} and V_{s30} bounds presented in Table 3 with a narrower M_w bound based on Bommer and Acevedo (2004) (i.e., [M_w −0.2, M_w +0.2]

Site condition V_{s30}=200 m/s

scenario	R_{rup}=5	R_{rup}=15	R_{rup}=30	R_{rup}=50	R_{rup}=80	R_{rup}=120
M_w=5.5	12	12	-	-	-	-
M_w=6.0	41	41	73	-	-	-
M_w=6.5	54	54	50	88	-	-
M_w=7.0	23	23	21	17	19	-
M_w=7.5	20	20	30	46	113	95
M_w=8.0	0	0	0	0	0	0

Site condition V_{s30}=400 m/s

scenario	R_{rup}=5	R_{rup}=15	R_{rup}=30	R_{rup}=50	R_{rup}=80	R_{rup}=120
M_w=5.5	55	55	-	-	-	-
M_w=6.0	187	187	294	-	-	-
M_w=6.5	109	109	175	296	-	-
M_w=7.0	52	52	45	57	79	-
M_w=7.5	77	77	60	141	228	158
M_w=8.0	1	1	1	3	4	5

Site condition V_{s30}=800 m/s

scenario	R_{rup}=5	R_{rup}=15	R_{rup}=30	R_{rup}=50	R_{rup}=80	R_{rup}=120
M_w=5.5	26	26	-	-	-	-
M_w=6.0	98	98	150	-	-	-
M_w=6.5	43	43	91	151	-	-
M_w=7.0	32	32	26	38	50	-
M_w=7.5	64	64	40	110	148	96
M_w=8.0	0	0	0	0	0	0

In contrast to the results presented in Table 5, Table 4 illustrated that utilizing 'wide' bounds on the causal parameters avoids an unreasonably small number of prospective ground motions for most of the considered scenario ruptures, with the exception of large magnitude ruptures (i.e., M_w7.5 and M_w8) with very short source-to-site distances (e.g., R_{rup}=5 and 15km) on soft soil (i.e., V_{s30}=200 m/s), where few observations exist. Based on Table 4 and Table 5 as well as the results presented by Tarbali and Bradley (2014a), the specific bounds presented in Table 3 are used in this study to select ground motion ensembles for scenario SHA. In regard to the above, it is important to note that the GCIM-based ground motion selection methodology uses multiple explicit IMs in order to account for various aspects of ground motions (i.e., amplitude, frequency content, duration, and cumulative effects), therefore, bounds on the causal parameters do not need to be overly restrictive.

2.3 Explicit intensity measures and the weight vectors considered

Within the framework of the GCIM methodology for ground motion selection, the following explicit IMs are considered: spectral acceleration for 18 vibration periods (T=0.05, 0.075, 0.1, 0.15, 0.2, 0.25, 0.3, 0.4, 0.5, 0.75, 1.0, 1.5, 2.0, 3.0, 4.0, 5.0, 7.5, and 10.0 s); peak ground acceleration (PGA); peak ground velocity (PGV); acceleration spectrum intensity (ASI); spectrum intensity (SI); displacement spectrum intensity (DSI); cumulative absolute velocity (CAV); and 5-75% and 5-95% significant durations (D_{s575} and D_{s595}, respectively). These IMs represent various aspects of ground motion severity: amplitude, frequency content, duration, and cumulative effects. The marginal distributions of these IMs for the considered rupture scenarios are obtained based on empirical ground motion prediction equations (GMPEs), namely: Boore and Atkinson (2008) for SA, PGA, and PGV; Bradley (2010b) for ASI; Bradley et al. (2009) for SI; Bradley (2011c) for DSI; Campbell and Bozorgnia (2010) for CAV; and Bommer et al. (2009) for D_{s575} and D_{s595}. Correlations between these IMs are considered based on existing empirical models (Baker and Jayaram 2008, Bradley et al. 2009, Bradley 2011b, Bradley 2011c, Bradley 2011a, 2012b, a).

As mentioned previously, causal parameters bounds are generally considered in ground motion selection in order to implicitly account for the different aspects of ground motions that are not represented by using only SA ordinates in the selection process. In order to illustrate the shortcomings of this approach, ground motion ensembles are first selected with and without causal parameter bounds based on considering only SA ordinates in the weight

vector of the GCIM method. This weight vector is denoted as 'SA only' in Table 6. The effect of the GCIM weight vector on the characteristics of selected ground motions are discussed thoroughly by Bradley (2012c) and Tarbali and Bradley (2014a, b), based on which the recommended weight vector implemented in this study contains IMs that represent amplitude, frequency content, duration, and cumulative effects of grounds motion, denoted as the 'generic' weight vector in Table 6.

Table 6: Weight vectors considered for ground motion selection

Weight vector	Amplitude and frequency content	Duration		Cumulative effects
	Spectral ordinates	D_{s575}	D_{s595}	CAV
SA only	1.0[1]	0.0	0.0	0.0
Generic	0.7[1]	0.1	0.1	0.1

[1]Evenly distributed over 18 *SA* ordinates, e.g., each SA ordinates has a weight of w_i =0.7/18 in the generic weight vector.

2.4 Characteristics of the selected ground motion ensembles

In this section, the explicit IM distributions of the selected ground motions with and without the application of causal parameter bounds are compared with the target GCIM distribution for the corresponding rupture scenarios. In addition, the distribution of implicit causal parameters of the selected ground motions (specifically, M_w, R_{rup}, and V_{s30}) are compared with those of the target scenario. A total of 20 ground motions are selected by conducting 10 replicate selections. More details regarding the number of replicate selections corresponding to the size of the ground motion ensemble are presented by Tarbali and Bradley (2014b).

2.4.1 Explicit intensity measures of selected ground motions—selection based on only SA ordinates

In order to illustrate the inadequacy of using causal parameter bounds to account for the shortcomings of selecting ground motions based on only SA ordinates, ground motion selection for the considered scenarios (see Table 2) is conducted with and without bounds based on only SA ordinates in the weight vector (see Table 6 for 'SA only' weight vector). Because ground motions are selected specifically to match the target SA ordinates then the selected ground motions have an appropriate representation of the target SA distribution for the whole range of vibration period considered (i.e., 0.05-10 s), and thus omitted for brevity. Figure 2 presents example results for the CAV and D_{s595} distribution of selected ground motions for several scenarios.

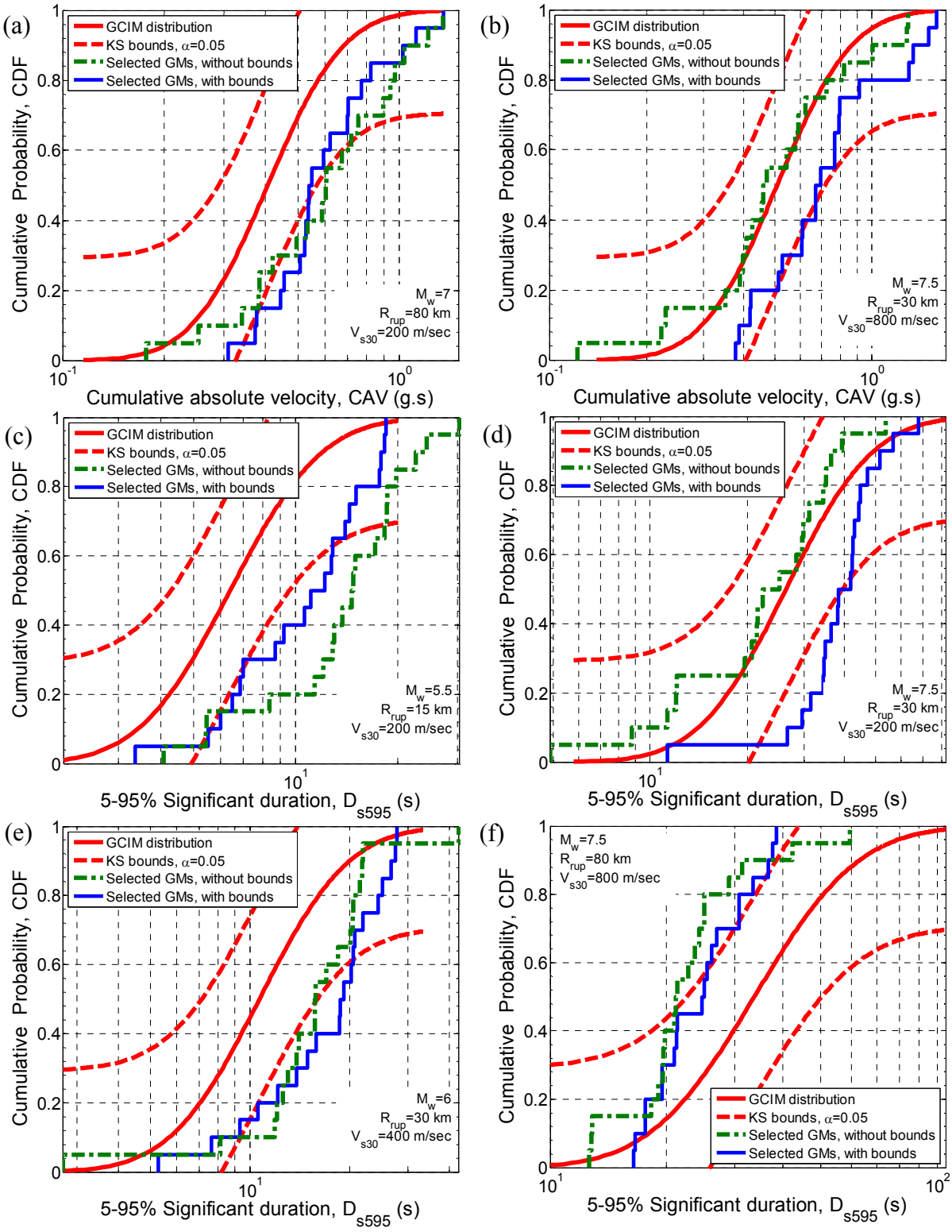

Figure 2: Bias in distribution of CAV and D_{s595} for different sample scenarios when ground motions are selected based on only SA ordinates and bounds are applied on the implicit causal parameters of prospective ground motions. Bias (at the $\alpha = 0.05$ significance level) is indicated when the empirical distribution of the selected motions lies outside the KS bounds of the target GCIM distribution.

Across the six example distributions shown Figure 2 it can be seen that in some cases the use of bounds makes no appreciable difference (e.g. Figure 2a, e, f); leads to mild improvement (e.g. Figure 2c); or results in a poorer empirical distribution (e.g. Figure 2Figure 2b, d) relative to the target distribution. In summary, comparing the selected motions based on the use of causal parameter bounds with the target CAV and D_{s595} distributions, it is clear that using causal parameter bounds cannot resolve the bias in distribution of these IMs of the selected ground motions. Although not presented here for brevity, bias is also evident in distribution of the other IMs such as D_{s575} for various scenarios.

The results presented in Figure 2 for sample rupture scenarios and site conditions illustrate that considering causal parameter bounds cannot strictly resolve the bias in distribution of IMs other than SA ordinates when ground motion selection is based solely on SA ordinates. As discussed thoroughly by Bradley (2012c) and Tarbali and Bradley (2014b), in order to avoid bias in the distribution of IMs that represent different aspects of ground motions, they need to be explicitly considered in the selection process by using an appropriate weight vector such as the 'generic' weight vector implemented in this study, as discussed in the next section.

2.4.2 Explicit intensity measures of selected ground motions—selection based on SA, duration, and cumulative effects

This section examines the effect of causal parameter bounds for ground motions selected based on the generic weight vector (see Table 6), which considers IMs for duration and cumulative effects along with the SA ordinates in the selection process. Figure 3 presents the characteristics of the ground motions selected for a sample scenario with M_w =6.5, R_{rup} =30 km, and V_{s30} =200 m/s. A total of N_{rec} =104 records are available for this specific scenario (as shown in Table 4) after the application of bounds, compared to 3222 available records when no bounds is applied, hence this scenario is an example where a relatively large number of prospective ground motions are available after the application of causal parameter bounds. Figure 3a-b present the acceleration response spectra of the individual ground motions selected without and with the application of causal parameter bounds along with the corresponding median, 16th, and 84th percentiles spectra representing the target SA distribution of the scenario. As illustrated in Figure 3a-b, using bounds on the causal parameters does not degrade the conformity of the selected ground motions to the target SA distribution. In addition, Figure 3c illustrates that the consideration of causal parameter bounds does not have a negative effect on the D_{s595} distribution of the selected ground

motions (nor the distributions of other non-SA IMs). Figure 3d presents the amplitude scaling factors of the selected ground motions with and without the application of causal parameter bounds. As shown, ground motions with smaller amplitude scaling factors are selected when causal parameter bounds are utilized in comparison to those obtained without the use of bounds. This is due to the fact that by restricting the prospective ground motions to motions with causal parameters similar to characteristics of the considered scenario, only a small change in amplitude of the as-recorded motions is required in order to represent the IM distributions for the considered scenario. As shown, most of the selected ground motions when using causal parameter bounds have a scaling factor within 0.3 to 3.0 range, which is similar to the desirable scaling range in seismic design guidelines (NZS1170.5 2004, ASCE/SEI7-10 2010).

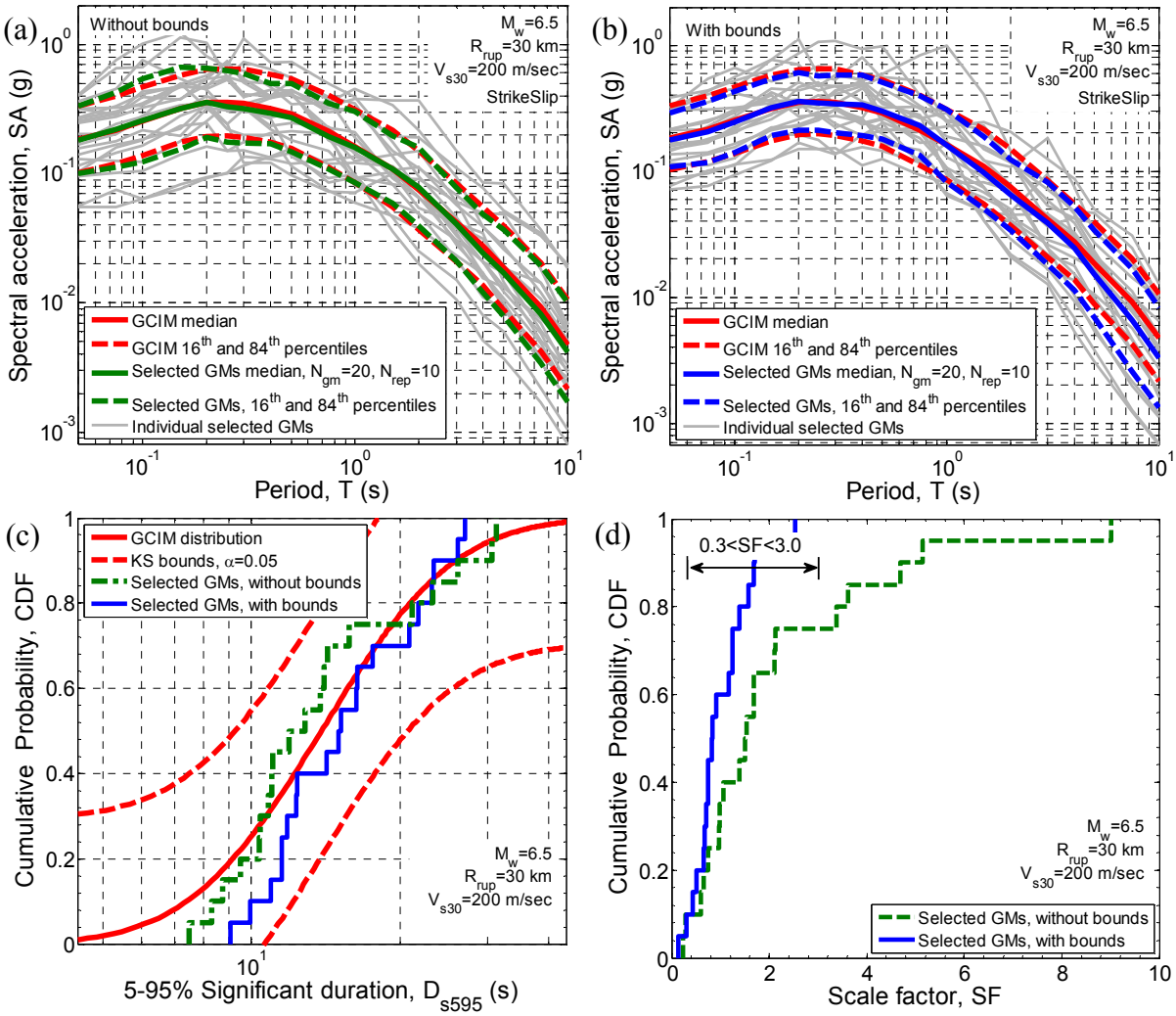

Figure 3: Properties of selected ground motions representing the M_w=6.5, R_{rup}=30 km, and V_{s30}=200 m/s scenario without and with the application of causal parameter bounds: (a) SA ordinates without bounds; (b) SA ordinates with bounds; (c) cumulative distribution of D_{s595}; (d) cumulative distribution of amplitude scaling factors.

Since the number of available ground motions for the M_w=6.5, R_{rup}=30 km, and V_{s30}=200 m/s scenario discussed in the previous paragraph was reasonably large (i.e., N_{rec}=104), the selected ground motion based on causal parameter bounds appropriately represent the target distribution of the considered IMs (Figure 3) and provide improved amplitude scale factors (i.e. closer to 1.0) than the selected motions without the use of causal parameter bounds. In contrast to the results presented in Figure 3, Figure 4 illustrates the characteristics of the selected ground motions to represent another scenario with M_w =7.5, R_{rup} =30 km, and V_{s30} =200 m/s, as an example among the scenarios for which there are relatively smaller number of ground motions available after applying bounds on the causal parameters (i.e., N_{rec} =30 for this specific scenario as presented in Table 4).

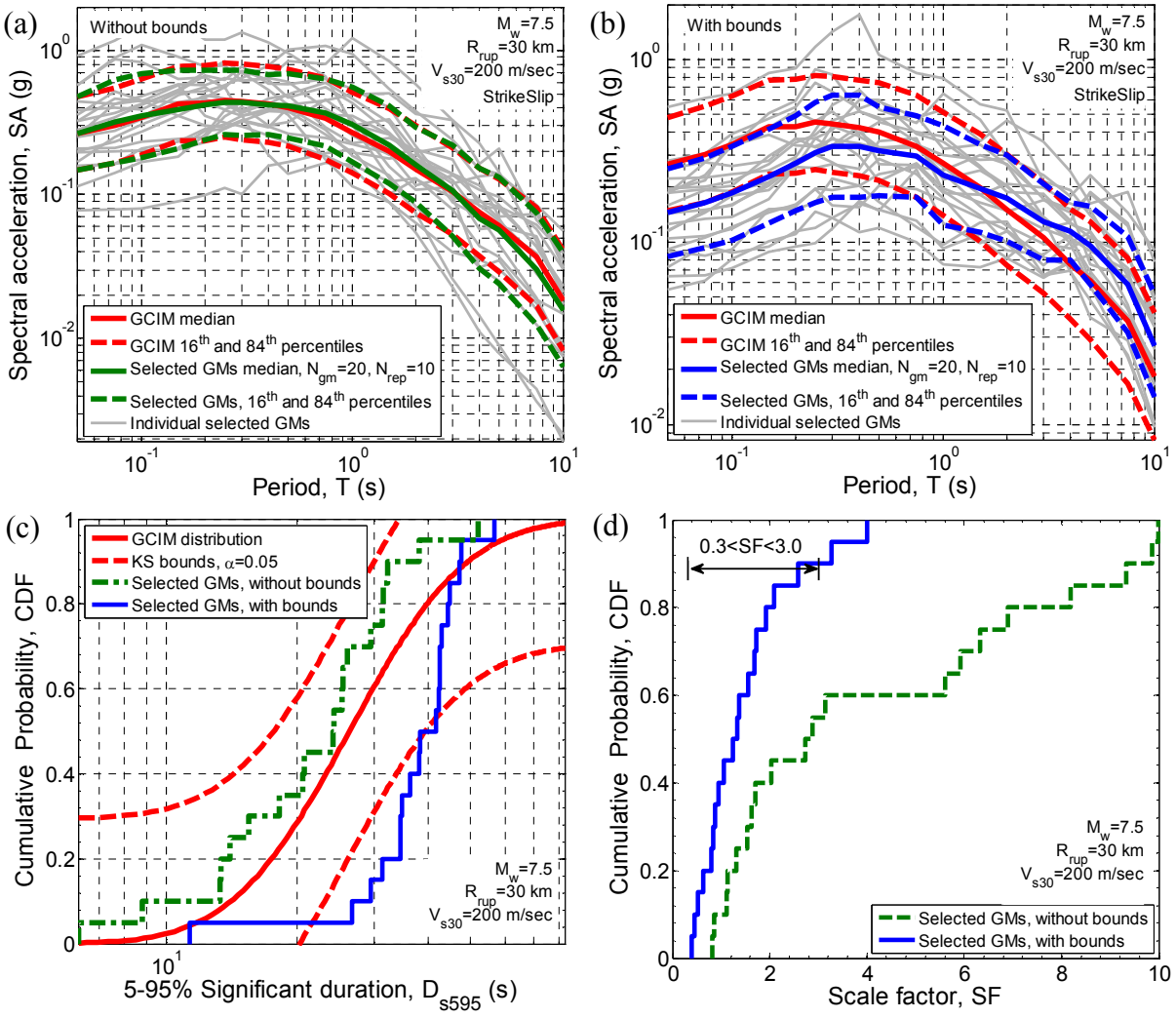

Figure 4: Properties of selected ground motions representing the M_w=7.5, R_{rup}=30 km, and V_{s30}=200 m/s scenario without and with the application of causal parameter bounds: (a) SA ordinates without bounds; (b) SA ordinates with bounds; (c) cumulative distribution of D_{s595}; (d) cumulative distribution of amplitude scaling factors

As shown in Figure 4a, the selected ground motions obtained without the use of causal parameter bounds do not have a biased representation of the SA or D_{s595} target distributions. However, the selected ground motions based on the use of causal parameter bounds are seen to exhibit bias in representing the target SA distribution across a wide range of vibration periods as well as the D_{s595} and the other IMs considered in the weight vector (i.e. D_{s575} and CAV). The poor representation of the target IM distributions for these selected ground motions can be attributed to the small number of prospective ground motions available after applying bounds on the causal parameters relative to the number of ground motions desired for selection (i.e., N_{rec}=30, of which 20 ground motions are desired), which is elaborated upon subsequently.

2.4.3 Overall representation of selected ground motion ensembles for all scenarios considered

The results presented in Figure 3 and Figure 4 illustrate the general trends relating to the characteristics of selected ground motions representing scenarios with large and small number of ground motions available after applying bounds on the causal parameters. In order to have an overall view on the obtained results for all of the considered scenario ruptures and site conditions, the global misfit of selected ground motion ensembles with and without bounds are compared in Figure 5 for each of the three different site conditions considered. As mentioned previously, the global misfit, R, indicates the consistency between the IM distributions of the selected ground motions and the target distribution based on the assigned weight on the IMs considered in the selection process.

It can be seen that for all three site conditions, for M_w≤7.0 there is practically no difference between the global misfit with or without bounds (i.e. the use of bounds does not lead to a degradation in the obtained ground motions with respect to the target IM distributions). In contrast, it can be seen that for the M_w7.5 and 8.0 scenarios the misfit for the selected motions when considering causal parameter bounds increases. This is most pronounced for the V_{s30}=200 m/s site condition, which has the smallest number of prospective ground motions (i.e., Table 4), and least pronounced for the V_{s30}=400 m/s site condition, which has the most prospective motions.

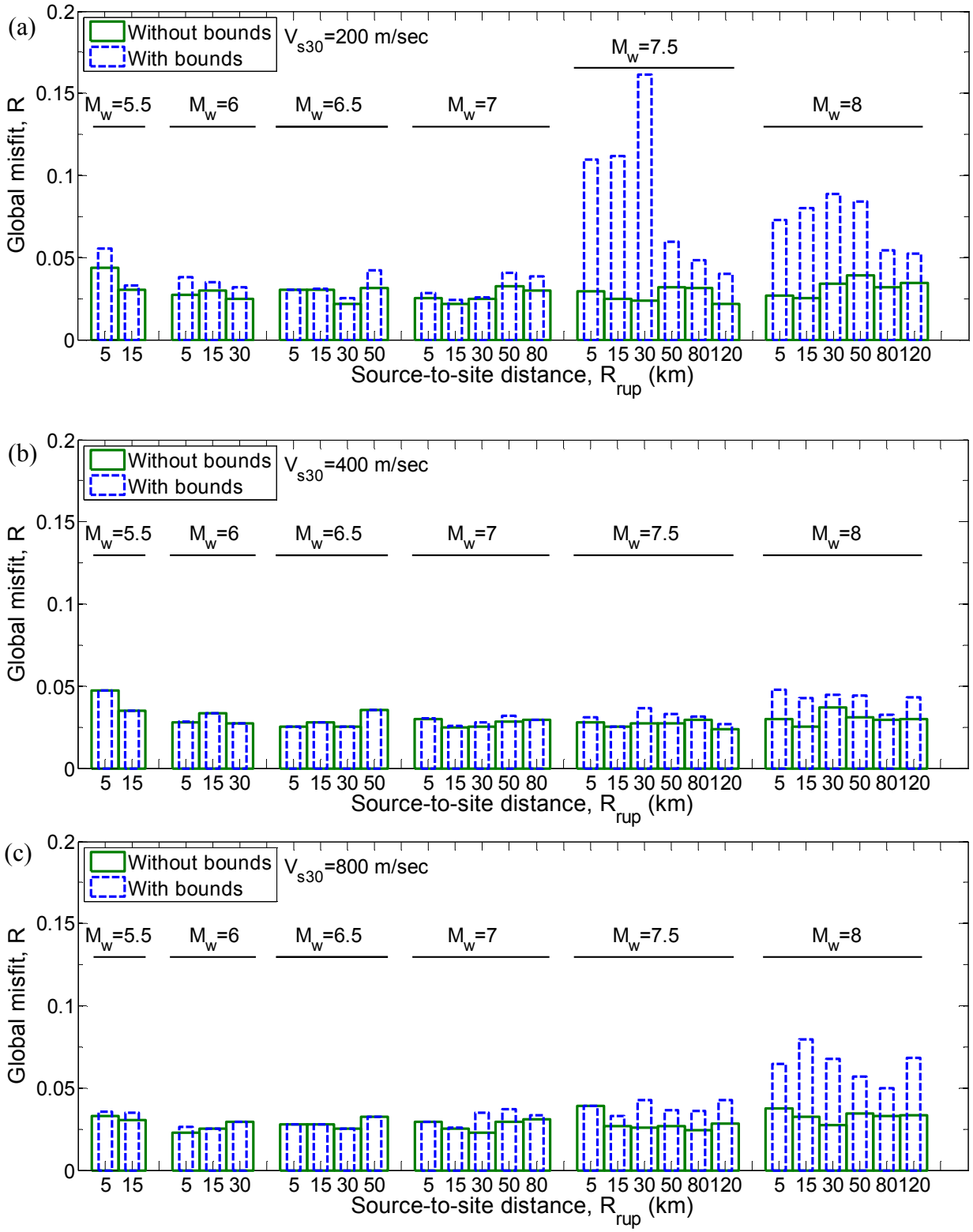

Figure 5: Global misfit of selected ground motion ensembles representing all of the considered rupture scenarios for three site conditions: (a) V_{s30}=200; (b) V_{s30}=400; and (c) V_{s30}=800 m/s.

By comparing the global misfit values for the M_w8.0 and 7.5 rupture scenarios with V_{s30} =200 m/s site condition (i.e., Figure 5a), it can be seen that the global misfits of selected

motions for the M_w7.5 rupture scenarios are higher than those for M_w8.0 scenarios, which may be initially counter-intuitive. This is caused by a large bias in the D_{s575} and D_{s595} distributions of selected ground motions compared to the target distribution. This principally occurs because the available ground motions after applying bounds for the M_w7.5 events (i.e., bounds of M_w=7.0-8.0 are predominantly from events with M_w>7.5 (so their D_{s575} and D_{s595} values are greater than the predicted distribution for M_w7.5 rupture scenarios). This is shown in Figure 4c, for example, where the median D_{s595} value of the selected ground motions is considerably larger than the median value of the target GCIM distribution. In contrast, ground motions from larger events in the M_w=7.5-8.5 are more suitable for the M_w8.0 rupture scenario, hence a smaller global misfit value for ground motion ensembles selected for M_w8.0 scenarios in Figure 5a.

2.4.4 Supplementing the NGA-West1 database with large magnitude recordings

In order to further examine the bias in the distribution of selected ground motions for M_w7.5 rupture scenarios when causal parameter bounds are applied, a few available ground motions from the NGA-West2 database (Ancheta et al. 2013) that are within the causal parameters bounds for M_w=7.5 rupture scenarios are added to the database of prospective ground motions. Table 7 compares the number of ground motions before and after adding ground motions to the NGA-West1 database (i.e., extended database) for M_w7.5 rupture scenarios. Using the extended database, ground motions are once again selected for M_w7.5 rupture scenarios with V_{s30} =200, 400, and 800 m/s site conditions.

Table 7: Number of available ground motion records (N_{rec}) for M_w7.5 scenario ruptures from the NGA-West1 and the extended databases after the application of the causal parameter bounds

Site condition V_{s30}=200 m/s							
	scenario	R_{rup}=5	R_{rup}=15	R_{rup}=30	R_{rup}=50	R_{rup}=80	R_{rup}=120
NGA-West1	M_w=7.5	22	22	30	47	119	119
Extended database	M_w=7.5	60	60	66	135	234	249
Site condition V_{s30}=400 m/s							
	scenario	R_{rup}=5	R_{rup}=15	R_{rup}=30	R_{rup}=50	R_{rup}=80	R_{rup}=120
NGA-West1	M_w=7.5	97	97	77	173	285	280
Extended database	M_w=7.5	143	143	122	239	367	429
Site condition V_{s30}=800 m/s							
	scenario	R_{rup}=5	R_{rup}=15	R_{rup}=30	R_{rup}=50	R_{rup}=80	R_{rup}=120
NGA-West1	M_w=7.5	76	76	47	124	171	127
Extended database	M_w=7.5	84	84	58	143	213	210

Figure 6 illustrates the characteristics of selected ground motions based on the extended database representing the M_w=7.5, R_{rup}=30 km, V_{s30}=200 m/s scenario, as an example among others. As presented in Table 7, the number of available ground motions for this specific scenario has been increased from 30 to 66. By comparing the results in Figure 6 with those presented in Figure 4 for the same scenario with the original NGA-West1 database, it can be seen that the additional prospective ground motions now lead to a subset of 20 selected ground motions without the bias in the distribution of SA ordinates and other considered IMs (i.e., CAV, D_{s595}, and D_{s575}). Also, the amplitude scaling factors of all of the selected ground motions are within 0.3 to 3.0 range.

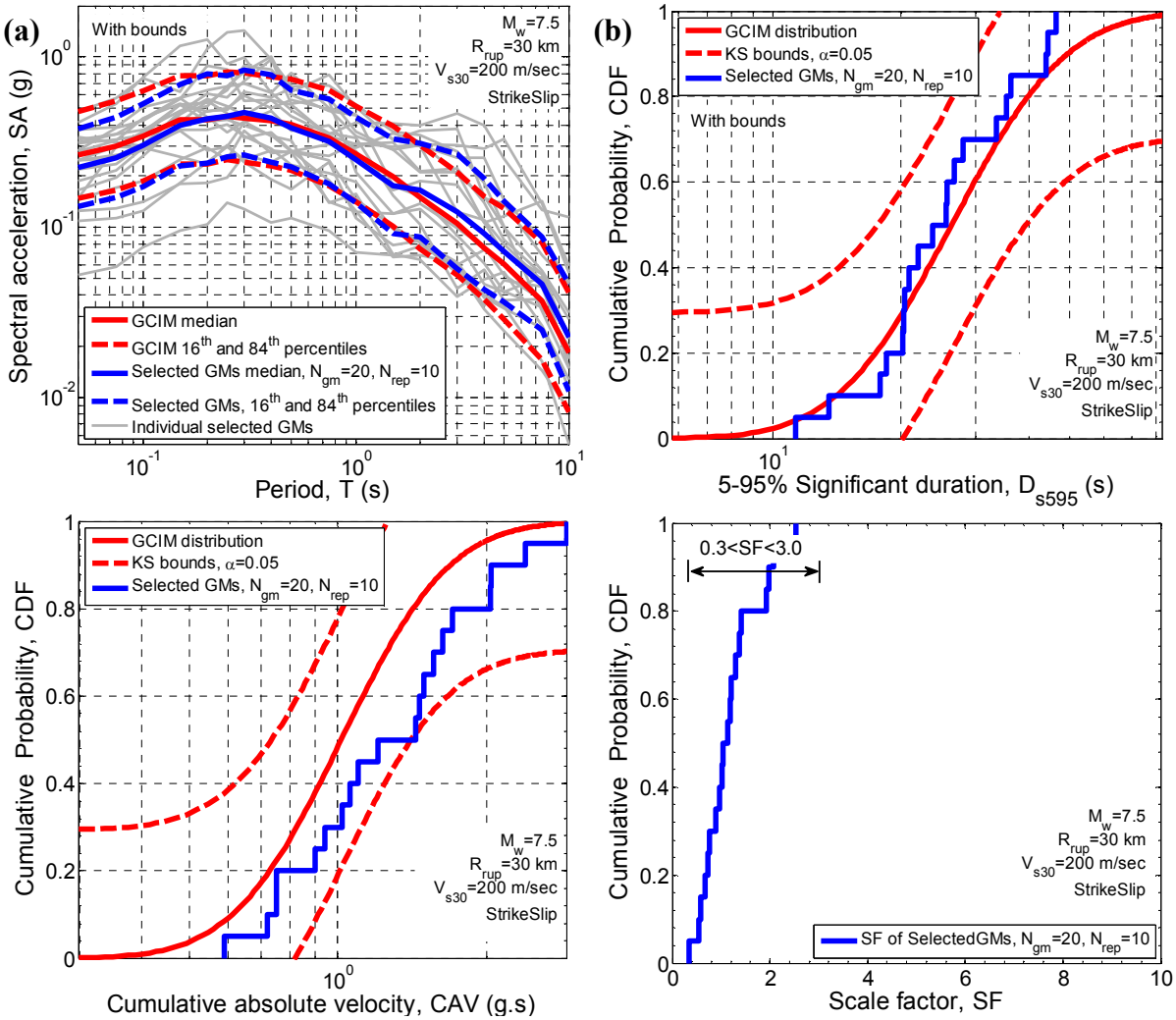

Figure 6: Properties of selected ground motions for M7.5R30V200 scenario with causal parameters bounds on the after adding extra ground motions from the NGA-West2 database: (a) SA ordinates; (b) D_{s595}; (c) CAV; (d) amplitude scaling factors.

In order to obtain an overall view on the effect of adding extra ground motions within the considered bounds for the M_w7.5 scenarios, Figure 7 compares the global misfits of the ground motions selected before and after extending the NGA-West1 database for M_w7.5 rupture scenarios (at 6 R_{rup} values) with V_{s30} =200, 400, and 800 m/s site conditions. As shown in Figure 7, the global misfit of selected ground motions based on causal parameter bounds have decreased, most significantly for the $V_{s30} = 200$m/s site condition. These reductions are consistent with the increase in the size of the prospective ground motions after the application of causal parameter bounds (i.e. Table 7), and clearly illustrate that the ability to obtain a set of selected ground motions with appropriate IM distributions (as reflected in the global misfit, R) is directly related to the number of prospective motions after the application of the causal parameter bounds relative to the number of desired ground motions. Based on the results presented here (i.e. for 20 desired ground motions) it is recommended that the number of prospective motions after the application of causal parameter bounds should be at least three times the desired number of ground motions (e.g. a minimum of 60 prospective motions if 20 selected motions are desired). If the use of a causal parameter bounds results in a small number of prospective ground motions relative to this factor of 3, then it is advised that the bound criteria are relaxed in order to avoid the selection of mis-representative ground motions (e.g., Figure 4).

Table 8 presents the available ground motions for the considered scenarios in this study from both the NGA-West1 and NGA-West2 databases. As illustrated in Table 8, the number of available ground motions for scenarios with $M_w \leq$7.5 for the three site conditions considered has significantly increased. However, for M_w8.0 scenarios with V_{s30}=200 and 800 m/s site conditions, the NGA-West2 database is still not well-constrained.

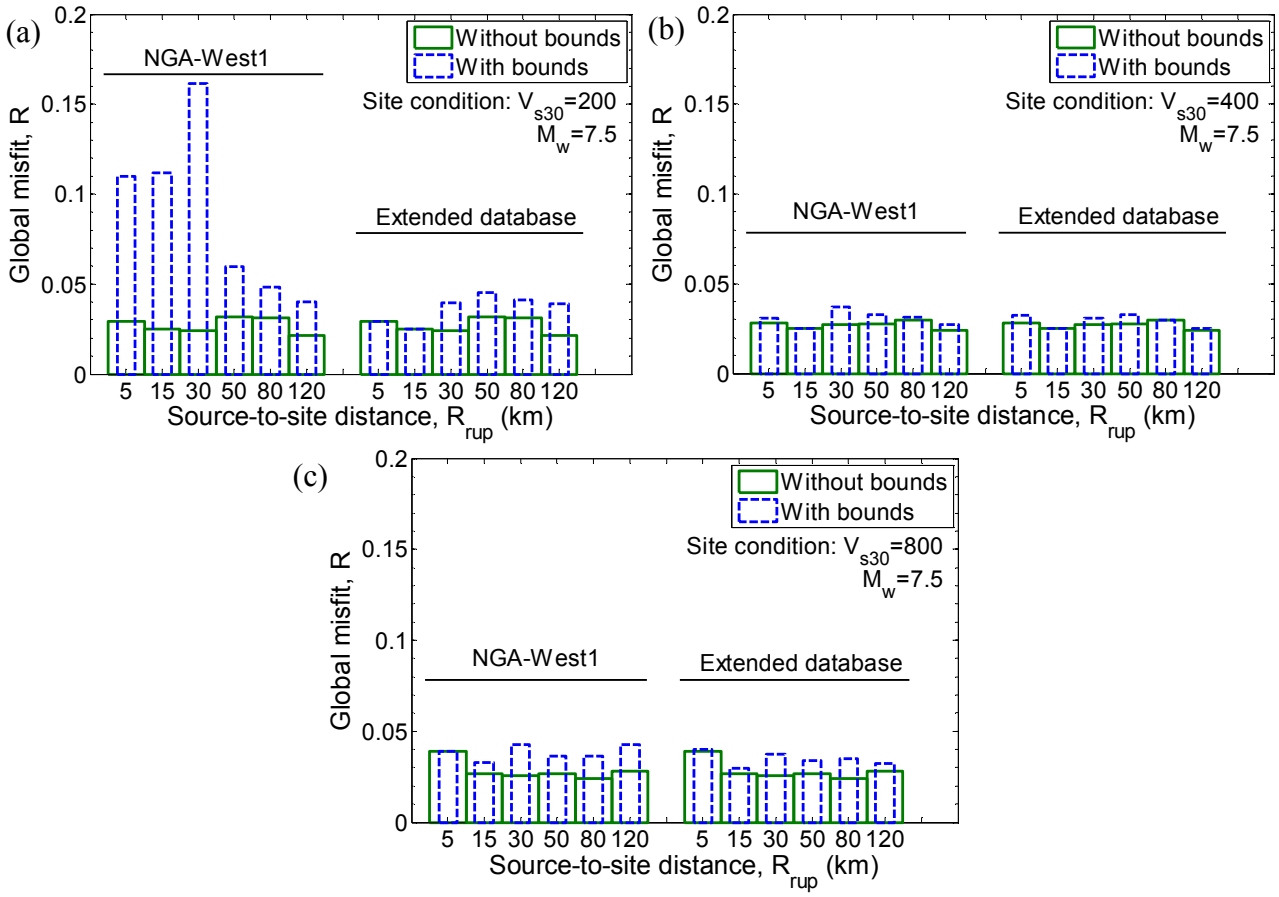

Figure 7: Global misfit of selected ground motions for M_w7.5 scenario ruptures based on the NGA-West1 and extended databases for the three considered site conditions: (a) V_{s30}=200 m/s; (b) V_{s30}=400 m/s; (c) V_{s30}=800 m/s.

Table 8: Comparison between the number of available ground motion records (N_{rec}) from the NGA-West1 and NGA-West2 databases based on the applied bounds for scenario-based ground motion selection cases considered

Site condition V_{s30}=200 m/s							
Scenario	NGA-West #	R_{rup}=5	R_{rup}=15	R_{rup}=30	R_{rup}=50	R_{rup}=80	R_{rup}=120
M_w=5.5	1	86	86	-	-	-	-
	2	146	146	-	-	-	-
M_w=6.0	1	66	66	108	-	-	-
	2	116	116	142	-	-	-
M_w=6.5	1	93	93	104	201	-	-
	2	187	187	173	305	-	-
M_w=7.0	1	68	68	48	54	55	-
	2	137	137	121	149	184	-
M_w=7.5	1	22	22	30	47	119	119
	2	60	60	67	79	144	142
M_w=8.0	1	20	20	30	39	105	93
	2	21	21	30	42	113	99
Site condition V_{s30}=400 m/s							
Scenario	NGA-West #	R_{rup}=5	R_{rup}=15	R_{rup}=30	R_{rup}=50	R_{rup}=80	R_{rup}=120
M_w=5.5	1	292	292	-	-	-	-
	2	575	575	-	-	-	-
M_w=6.0	1	268	268	409	-	-	-
	2	446	446	573	-	-	-
M_w=6.5	1	234	234	349	667	-	-
	2	458	458	544	1001	-	-
M_w=7.0	1	145	145	143	195	210	-
	2	284	284	305	470	659	-
M_w=7.5	1	97	97	77	173	285	280
	2	164	164	135	264	408	475
M_w=8.0	1	76	76	59	126	211	152
	2	92	92	71	150	250	196
Site condition V_{s30}=800 m/s							
Scenario	NGA-West #	R_{rup}=5	R_{rup}=15	R_{rup}=30	R_{rup}=50	R_{rup}=80	R_{rup}=120
M_w=5.5	1	128	128	-	-	-	-
	2	271	271	-	-	-	-
M_w=6.0	1	134	134	210	-	-	-
	2	231	231	282	-	-	-
M_w=6.5	1	124	124	204	445	-	-
	2	243	243	331	630	-	-
M_w=7.0	1	68	68	68	83	89	-
	2	145	145	172	243	347	-
M_w=7.5	1	76	76	47	124	171	127
	2	101	101	68	153	239	246
M_w=8.0	1	61	61	40	109	147	95
	2	73	73	50	119	171	129

2.4.5 Implicit causal parameters of selected ground motions

In addition to the distribution of explicit IMs discussed above, considering bounds on the causal parameters affects the causal parameter distribution of the selected ground motions, which is worthy of investigation. Figure 8 presents the $M_w - R_{rup}$ distribution of the selected ground motions representing four sample scenarios as noted in the figure insets. Due to the large number of considered rupture scenarios, the presented results depicted here were chosen to illustrate the trend in all of the considered cases. Figure 8a provides an example for scenarios with very small source-to-site distances (i.e., 5 and 15 km), in which it can be seen that the R_{rup} values of the selected ground motions without bounds are distributed over a wide range and are mostly larger than that of the target scenario, whereas it can be seen that the application of causal parameter bounds leads to an improved representation of the target R_{rup} values (and also a minor improvement in the M_w distribution). In general, having a small number of prospective ground motions in the near-fault region prevents from selecting ground motions that closely encompass the target scenario R_{rup}.

Figure 8b compares the M_w-R_{rup} distribution of the selected ground motions without and with bounds for the M_w=6.5, R_{rup}=50 km, V_{s30}=400 m/s scenario, as an example for scenarios with large number of ground motions after the application of causal parameter bounds (i.e., N_{rec}=667 for this specific scenario as presented in Table 4). As shown in Figure 8b, the causal parameters of the selected ground motions can appropriately represent the target scenario causal parameters, with mean R_{rup} and M_w values close to the target scenario characteristics. It is noted that for ground motions selected without bounds, the R_{rup} and M_w values of the selected motions are distributed over a very wide range as shown in Figure 8b (i.e., M_w =[5.5, 7.6]; and R_{rup}=[0.2, 200]), whereas the ground motions selected based on the bounds are distributed in a narrower range around the scenario parameters.

As an example for scenarios with large magnitudes (i.e., $M_w \leq 7.5$) and large source-to-site distances (i.e., $R_{rup} \geq 80$), Figure 8c shows the M_w-R_{rup} distribution of the selected ground motions for the M_w=7.5, R_{rup}=120 km, V_{s30}=400 m/s scenario. As illustrated, ground motions selected after applying bounds have a significantly improved representation of the M_w and R_{rup} value of the target scenario. As illustrated in Figure 8a-c, ground motions selected based on bounds for scenarios with $M_w \leq 7.5$ have an appropriate representation of the target scenario magnitude. In contrast, as shown in Figure 8d for scenarios with very large

rupture magnitude (e.g., M_w=8.0), the causal magnitudes of the selected ground motions are mostly below the target scenario magnitude due to a paucity of recorded ground motions from events with such large magnitudes.

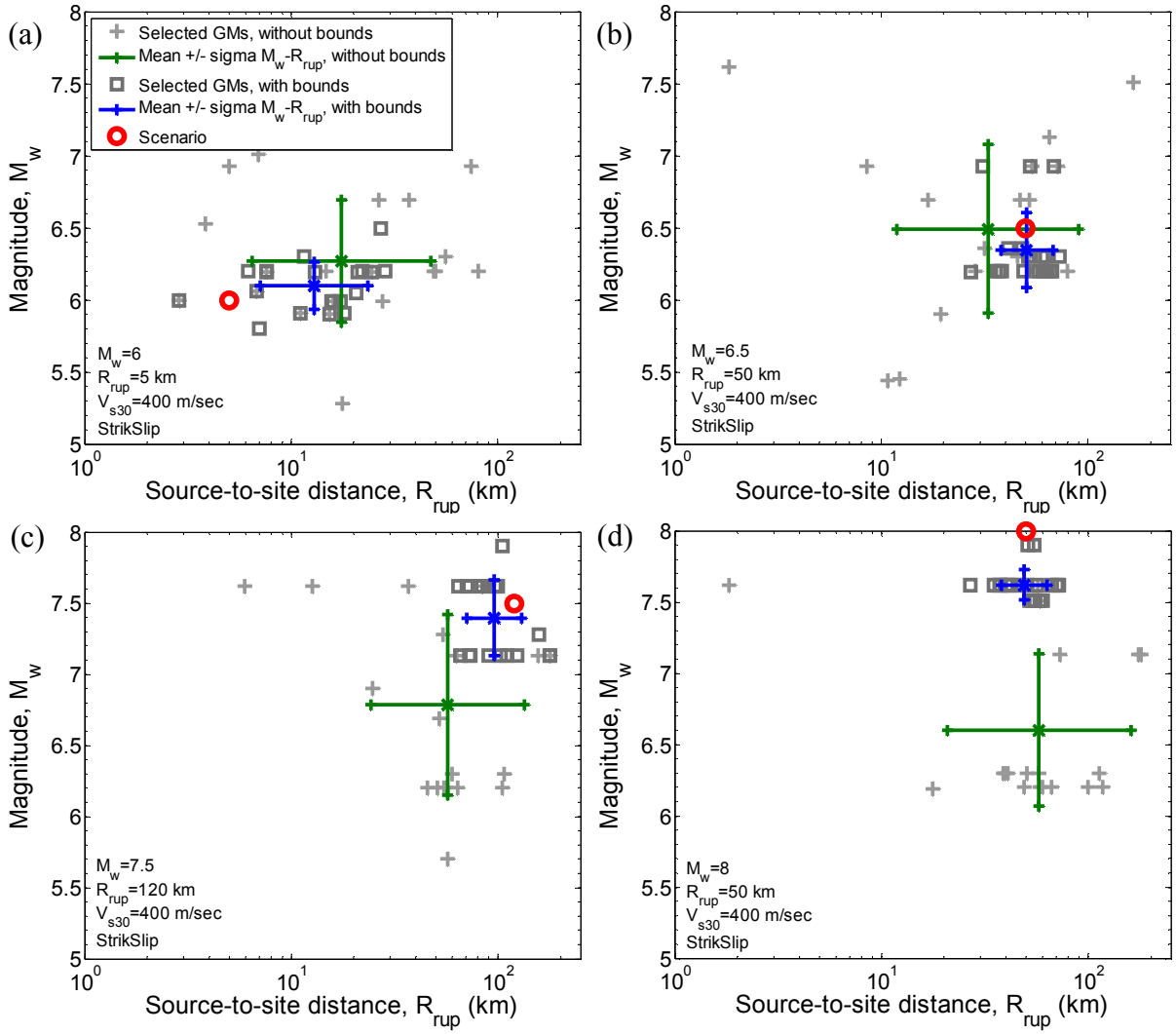

Figure 8: Comparison between M_w-R_{rup} distribution of selected ground motions with and without bounds for sample scenarios (scenario details shown in figure insets).

In order to compare the site condition of selected ground motions with and without the application of bounds on the causal parameters, Figure 9 presents the V_{s30}-R_{rup} distribution of the selected ground motions for M_w=7.0, R_{rup}=50 km scenario ruptures, as an example among others, with V_{s30}=200, 400, and 800 m/s site conditions. As shown in Figure 9a for soft soil conditions (i.e., V_{s30}=200 m/s), the selected ground motions without bounds have V_{s30} values distributed over a wide range, with ground motions recorded on rock (i.e., V_{s30} ≥800 m/s) being selected. In contrast, when bounds are applied on the causal parameters, the V_{s30} values of the selected ground motions are consistent with the considered

site condition (see Figure 9a). This also holds true for stiff soil deposit (i.e., V_{s30}=400 m/s) as shown in Figure 9b, although the selected ground motions without the consideration of bounds have a more reasonable V_{s30} distribution compared to that for the V_{s30}=200 m/s site condition because of the larger number of prospective ground motions recorded on stiff soil deposits. Figure 9c illustrates that the ground motions selected for the soft rock site have V_{s30} values below that of the target site (V_{s30}=800 m/s). While the use of causal parameter bounds on V_{s30} improves the distribution of V_{s30} values of the selected ground motions, they are still, on average, below 800m/s simply because of the paucity of as-recorded ground motions on rock conditions.

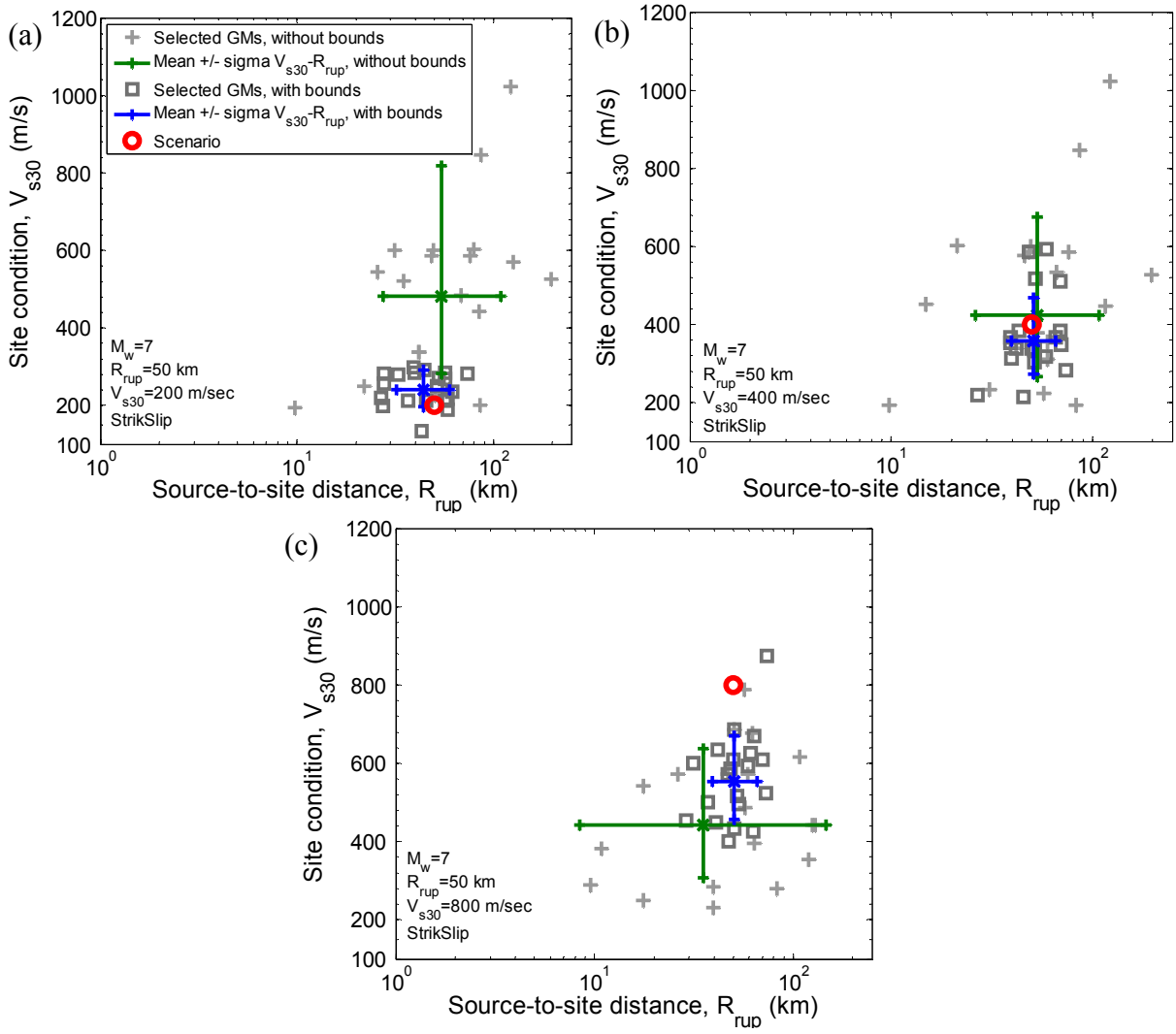

Figure 9: Comparison between V_{s30}-R_{rup} distribution of selected ground motions with and without bounds representing a M_w=7 R_{rup}=50 km sample scenario with three site conditions: (a) V_{s30}=200 m/s; (b) V_{s30}=400 m/s; (c) V_{s30}=800 m/s.

2.4.6 Magnitude-distance-site class distributions of the NGA-West1 and NGA-West2 databases

In order to compare the site class distribution in empirical ground motion databases for different site conditions, Table 9 presents the number of available ground motions in the NGA-West1 and NGA-West2 databases for four site classes (i.e., A/B, C, D, and E) based on the NEHRP (2003) guidelines. As presented in Table 9, ground motions recorded on site class A/B (i.e., $V_{s30} \geq$760 m/s) and site class E (i.e., $V_{s30} \leq$180 m/s) represent very small portions of these empirical ground motion databases. On the other hand, it can be seen that a significant improvement in the number of as-recorded ground motions for site class A/B and also site classes C and D has taken place in the NGA-West2 database compared to the NGA-West1 database.

Table 9: Number of available ground motions in the NGA-West1 and NGA-West2 databases within the NEHRP (2003) site classes for the whole range of M_w and R_{rup}

	Site class E V_{s30}=(0,180]	Site class D V_{s30}=(180,360]	Site class C V_{s30}=(360,760]	Site class A/B V_{s30}=[760, inf)
NGA-West1*	54 (<2%)	1665 (52%)	1427 (44%)	79 (<2%)
NGA-West2**	196 (<1%)	6827 (32%)	13234 (62%)	1199(6%)

* based on the flat-file available at http://peer.berkeley.edu/ngawest/activity_findings.html
** based on the flat-file available at http://ngawest2.berkeley.edu/site/documentation

Figure 10 illustrates the $M_w - R_{rup}$ distribution of the recordings from the NGA-West1 and NGA-West2 databases for three NEHRP (2003) site classes, namely site classes A/B, C, and D (but not E since the number of recordings is small as shown in Table 9). As shown in Figure 10b, despite the significant growth in the number of recordings, most of the ground motions in the NGA-West2 database with site class A/B have M_w<5.0, which are often not of engineering interest for ground motion selection. Figure 10a-b illustrates that ground motions with $M_w \geq$5.0 from site class A/B are relatively sparse over the whole M_w and R_{rup} range in both databases. In contrast, as shown in Figure 10c-f, ground motions recorded on site class C and D cover a large range of M_w and R_{rup} in both databases. Figure 10 also illustrates that neither of the NGA databases are well-constrained for ground motions with $M_w \geq$7.0 in the near-fault region ($R_{rup} \leq$ 30 km).

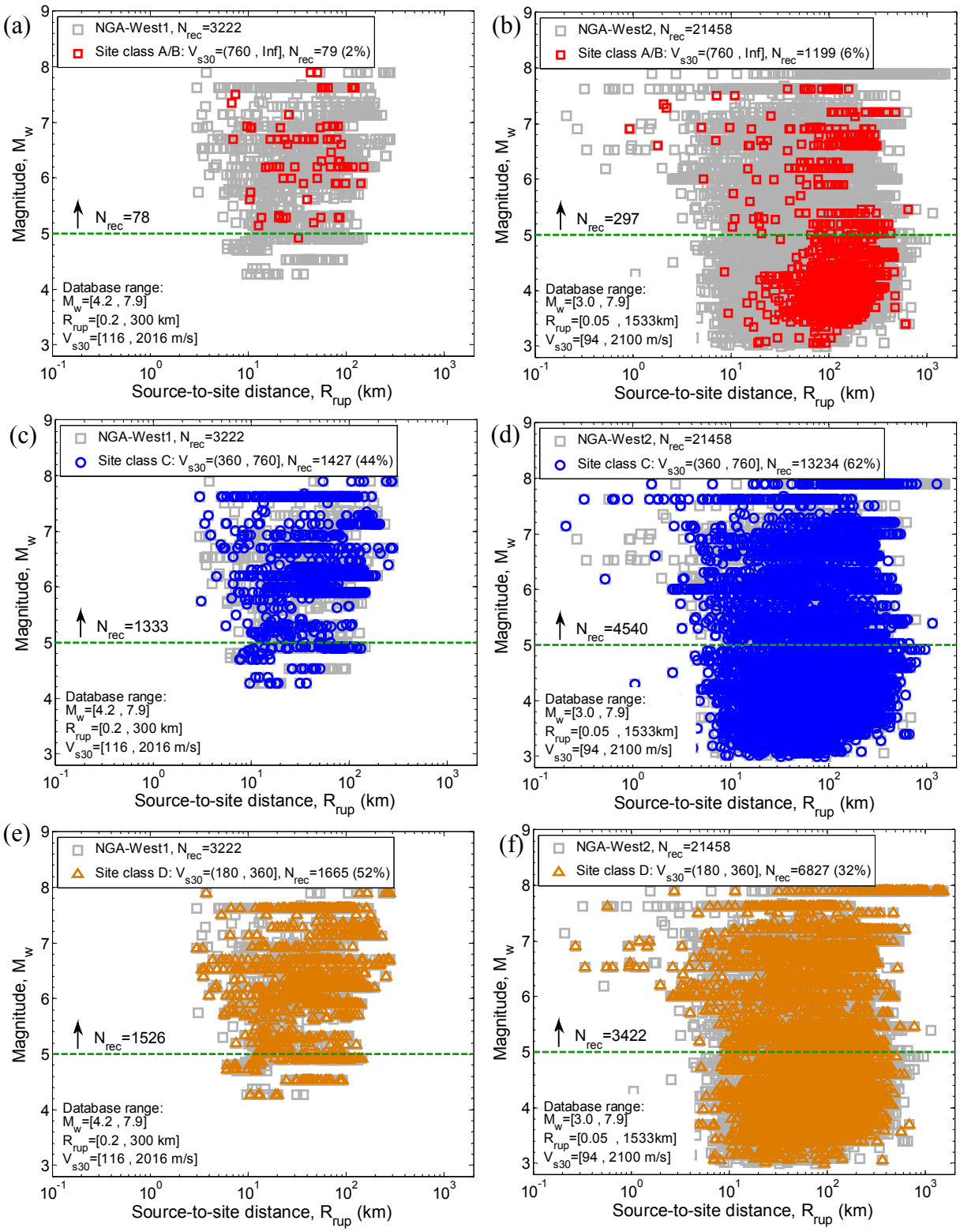

Figure 10: M_w-R_{rup} distribution of ground motions from the NGA-West1 and NGA-West2 databases for three different site classes based on the NEHRP (2003) guidelines: (a)-(b) site class A/B; (c)-(d) site class C; (e)-(f) site class D.

Comparison between the NGA-West1 and NGA-West2 databases for ground motions with M_w ≥5.0, as presented in Table 10, reveals that the number of ground motions for site class A/B has increased from 78 to 297, which provides a notably improved database for conducting ground motion selection for rock sites. Also the number of ground motions with M_w ≥5.0 has increased significantly in the NGA-West2 databases for site class C and D, except in the near-fault region (R_{rup} ≤ 30 km) for recordings with M_w ≥7.0. As presented in Table 8 despite the significant improvement in number of the ground motions in the NGA-West2 database, the number of the available records based on the applied bounds for ground motion selection representing scenario ruptures with M_w ≥7.5 at short-to-moderate source-to-site distances (i.e., R_{rup} ≤50 km) is still small, especially for soft soil and soft rock site conditions (i.e., V_{s30}=200 and 800 m/s).

Table 10: Comparison between the number of available ground motions with M_w≥5 in the NGA-West1 and NGA-West2 databases based on the NEHRP (2003) site classes

	Site class E/F V_{s30}=(0,180]	Site class D V_{s30}=(180,360]	Site class C V_{s30}=(360,760]	Site class A/B V_{s30}=[760, inf)
NGA-West1*	53 (<2%)	1526 (47%)	1333 (41%)	78 (<2%)
NGA-West2**	191 (<1%)	3422 (<16%)	4540 (21%)	297 (<1%)

* based on the flat-file available at http://peer.berkeley.edu/ngawest/activity_findings.html
** based on the flat-file available at http://ngawest2.berkeley.edu/site/documentation

2.5 Effect of causal parameter bounds on the computational efficiency of scenario-based ground motion selection

The computational cost of ground motion selection is an important issue when selecting ground motion ensembles representing scenario SHA. As elaborated by Tarbali and Bradley (Tarbali and Bradley 2014b), selecting ground motions to represent target distribution of IMs for a scenario SHA requires calculating optimum amplitude scaling factors for all prospective ground motions included in the database. Therefore, reducing the number of prospective ground motions by considering causal parameter bounds increases the computational efficiency of the selection process. As an illustration, Figure 11 compares the computational cost of conducting ground motion selections with and without causal parameter bounds for all of the considered scenario ruptures and site conditions in this study. The computational cost is measured based on the time spent to select an ensemble of 20 ground motions by conducting 10 replicate selections using a typical desktop computer (i.e., a Pentium 4 processor with a 2.93 GHz CPU and 4GB RAM).

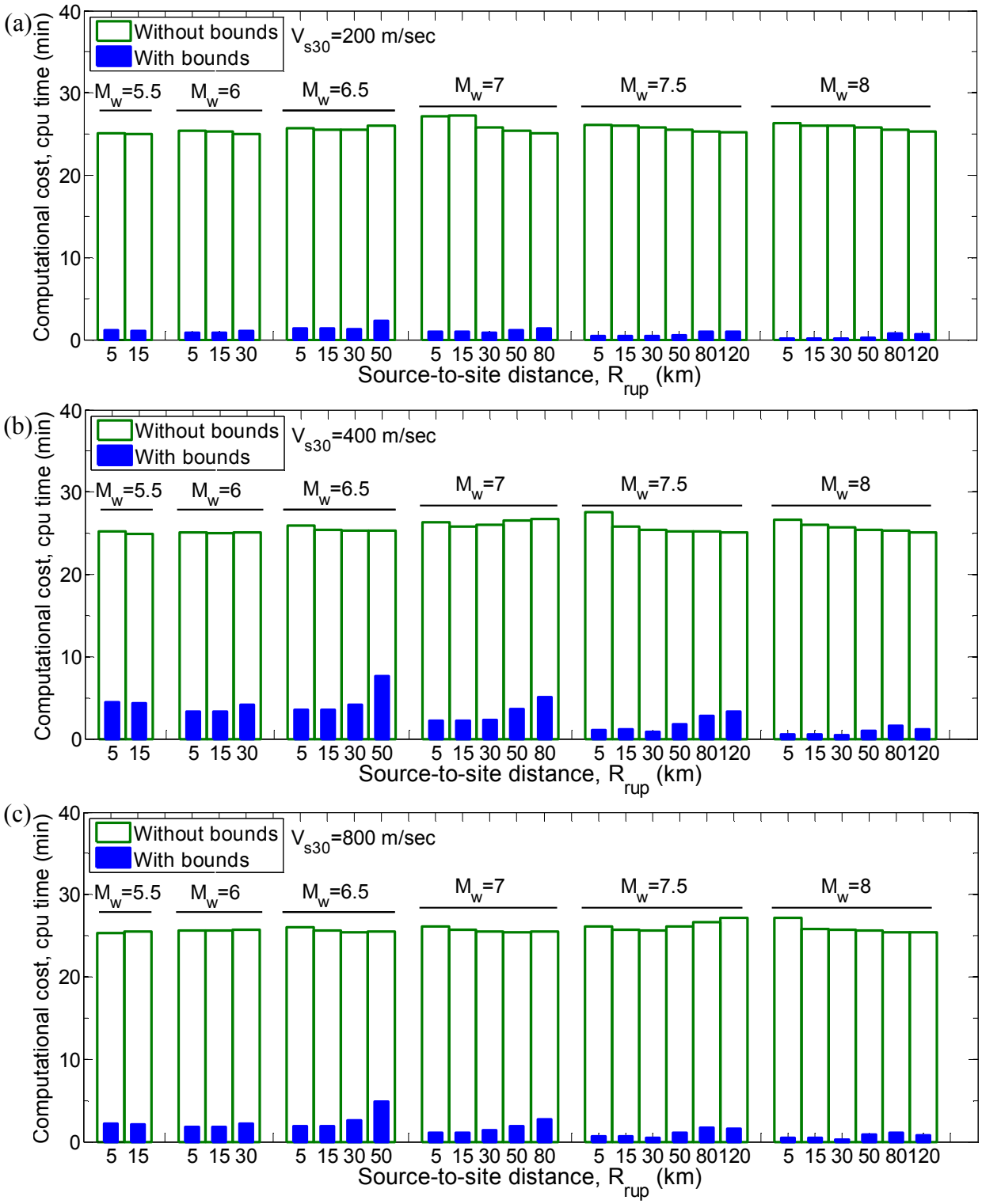

Figure 11: Comparison between the computational cost of scenario-based ground motion selection with and without causal parameters bounds for the considered scenario ruptures on three site conditions: (a) V_{s30}=200 m/s; (b) V_{s30}=400 m/s; (c) V_{s30}=800 m/s.

As shown in Figure 11, selecting ground motions from the NGA-West1 database with 3222 available ground motions when no causal parameter bounds are applied takes over 25 minutes of computation time, whereas, by using bounds on the causal parameters, the number

of the prospective ground motions reduces to a reasonable number and the selection process requires less than 5 minutes for most of the considered scenarios. It can also be seen that ground motion selection based on causal parameter bounds for V_{s30}=400 m/s scenarios requires longer computational times than that for V_{s30}=200 and 800 m/s scenarios, due to a larger number of records available for V_{s30}=400 m/s scenarios (see Table 4). It is obvious that in case of using a larger number of replicate selections to select an ensemble of ground motions (Tarbali and Bradley 2014b) or utilizing a database with a large number of prospective ground motions outside of the considered causal parameter bounds, the difference between the computational time of ground motion selection with and without the application of bounds will be even more accentuated.

3 Ground-motion selection for probabilistic seismic hazard analysis (PSHA)

Probabilistic seismic hazard analysis (PSHA) represents the integrated hazard from all possible scenario ruptures in the vicinity of the site by considering the likelihood of the occurrence of each scenario. Assessing the performance of engineered systems against a probabilistic seismic hazard via dynamic response analysis requires selecting ground motions ensembles representing the desired probabilistic hazard level. Bradley (2012c) developed the GCIM ground motion selection methodology to holistically select ground motions based on PSHA results. In this methodology, the target for ground motion selection is based on the distribution of multiple IMs (which accounts for various aspects of ground motion severity), and incorporates the contribution of all scenario ruptures affecting the seismic hazard based on deaggregation results. Similar to the scenario-based ground motion selection in the previous sections, a weight vector is implemented to allocate the relative importance of the considered IMs (Bradley 2012c), and the global misfit, i.e., Equation (1), is used to assess the overall representation of the selected ground motions to the target IM distributions (Bradley 2013).

In the following section, various PSHA cases with noticeably different deaggregation distributions are used to determine appropriate causal parameter bounds on magnitude and source-to-site distance. Subsequently, the impact of alternative proposals for causal parameter bounds on the characteristics of the selected ground motions are investigated and the pertinent implications presented.

3.1 Seismic hazard cases and site conditions considered

In order to investigate the effect of various causal parameter bounds on the characteristics of ground motions selected for PSHA cases with different deaggregation distributions, PSHA was conducted for numerous SA vibration periods and sites in California, U.S., using the open-source seismic-hazard analysis software OpenSHA (Field et al. 2003). The earthquake rupture forecast of Petersen et al. (2007) and empirical ground motion prediction and correlation models presented in section 2.3 were used to conduct PSHA and obtained the GCIM distributions of the considered IMs. 12 PSHA cases are considered here which are intentionally chosen to span a wide range of deaggregation conditions in order to examine in detail the subsequently presented proposals for causal parameter bounds. It is noted that each PSHA was conducted for three site conditions with V_{s30}=200, 400 and 800 m/s, i.e., a total of 36 PSHA-based ground motion selection cases. Table 11 presents details regarding the considered PSHA cases, including the location, site condition, conditioning IM, and hazard level. Also, Figure 12 illustrates the deaggregation results for the 12 PSHA cases corresponding to the V_{s30}=200 m/s site condition, with PSHAs for the V_{s30}=400 and 800 m/s site conditions result in similar deaggregation distributions, and are therefore omitted for brevity. It can be seen in Figure 12 that these 12 cases span a wide range of causal parameter distributions, including: (i) large M_w scenarios and small R_{rup} values in the near-fault region (i.e., cases 1-5); (ii) large variability in M_w and R_{rup} of the contributing scenarios (i.e., cases 6-8); (iii) dominant scenarios with small, moderate, or large R_{rup} values (i.e., cases 9-12).

Table 11: Characteristics of the considered 12 PSHA cases for each site condition in order to examine different causal parameters bounds on M_w and R_{rup}

PSHA case	Site	Latitude, Longitude	Site condition, V_{s30}(m/s)	Conditioning IM	Hazard level in 50 years
1	Stanford	37.4225, -122.1653	200, 400, 800	SA(0.5s)	2%
2	San Francisco	37.7833, -122.4167	200, 400, 800	SA(0.5s)	2%
3	Stanford	37.4225, -122.1653	200, 400, 800	SA(0.5s)	50%
4	Los Angeles	34.05, -118.25	200, 400, 800	SA(0.5s)	2%
5	San Francisco	37.7833, -122.4167	200, 400, 800	SA(0.5s)	50%
6	Los Angeles	34.05, -118.25	200, 400, 800	SA(0.5s)	50%
7	Sacramento	38.5556, -121.4689	200, 400, 800	SA(0.5s)	2%
8	Davis	38.5539, -121.7381	200, 400, 800	SA(0.5s)	50%
9	Davis	38.5539, -121.7381	200, 400, 800	SA(0.5s)	2%
10	Los Angeles	34.05, -118.25	200, 400, 800	SA(3.0s)	50%
11	Los Angeles	34.05, -118.25	200, 400, 800	SA(3.0s)	2%
12	Davis	38.5539, -121.7381	200, 400, 800	SA(3.0s)	2%

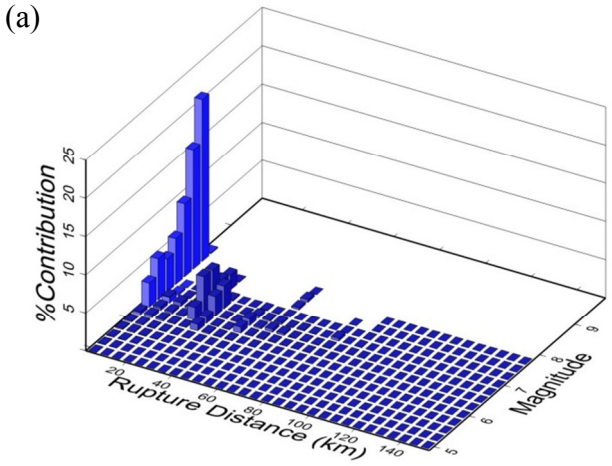

Case 1: Stanford: SA(0.5s) for a 2% in 50 yrs hazard

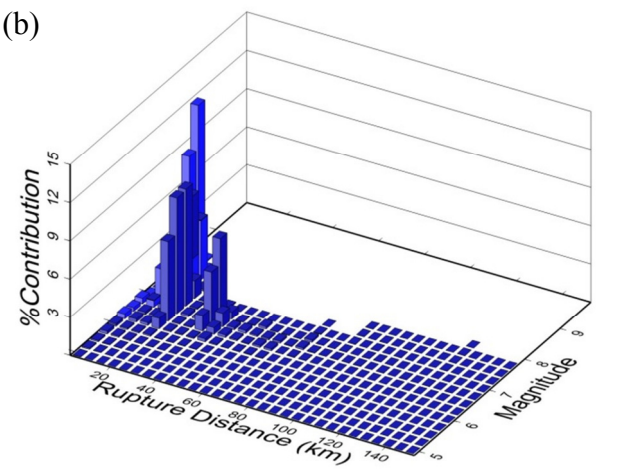

Case 2: San Francisco: SA(0.5s) for a 2% in 50 yrs hazard

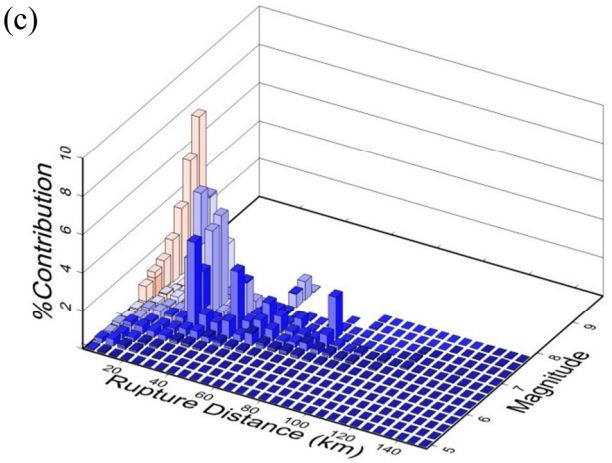

Case 4: Stanford: SA(0.5s) for a 50% in 50 yrs hazard

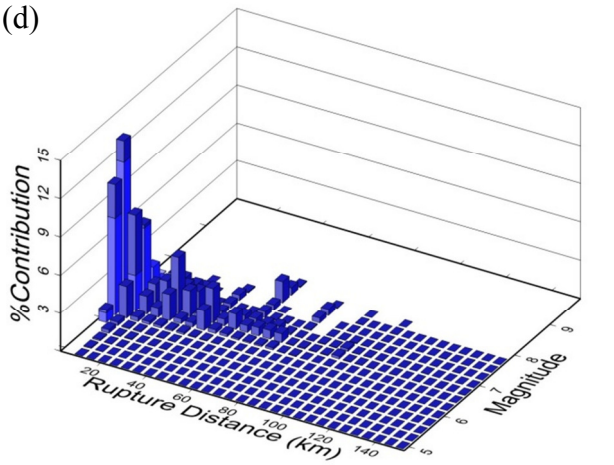

Case 5: Los Angeles: SA(0.5s) for a 2% in 50 yrs hazard

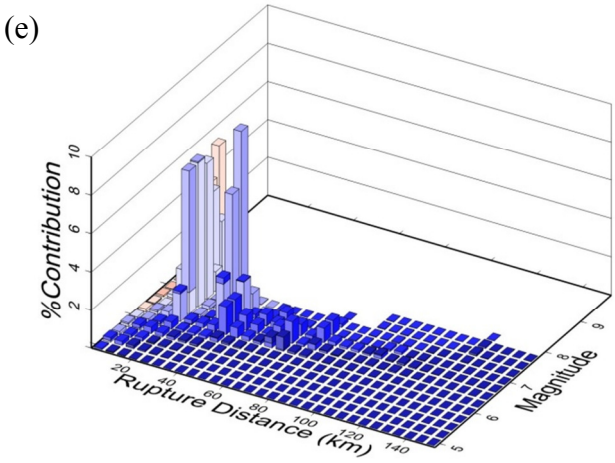

Case 5: San Francisco: SA(0.5s) for a 50% in 50 yrs hazard

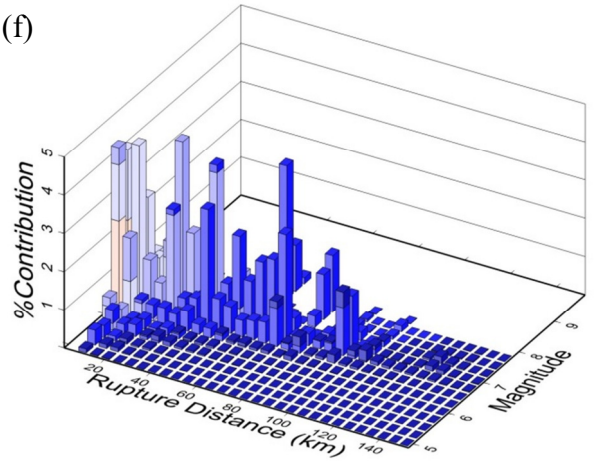

Case 6: Los Angeles: SA(0.5s) for a 50% in 50 yrs hazard

Figure 12: Deaggregation distribution of the 12 PSHA cases with the Vs30=200 m/s site condition: (a) Stanford, SA(0.5s) hazard for a 2% probability in 50 years; (b) San Francisco, SA (0.5s) hazard for a 2% in 50 years; (c) Stanford, SA (0.5s) hazard for a 50% in 50 years; (d) Los Angeles, SA (0.5s) hazard for a 2% in 50 years; (e) San Francisco, SA (0.5s) hazard for a 50% in 50 years; (f) Los Angeles, SA(0.5s) hazard for a 50% in 50 years.

(g)

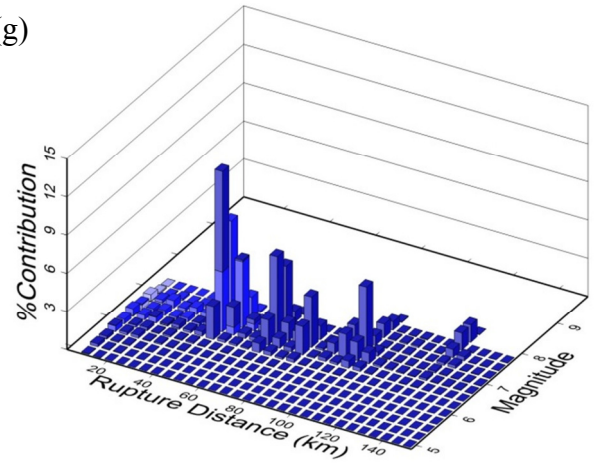

Case 7: Sacramento: SA(0.5s) for a 2% in 50 yrs hazard

(h)

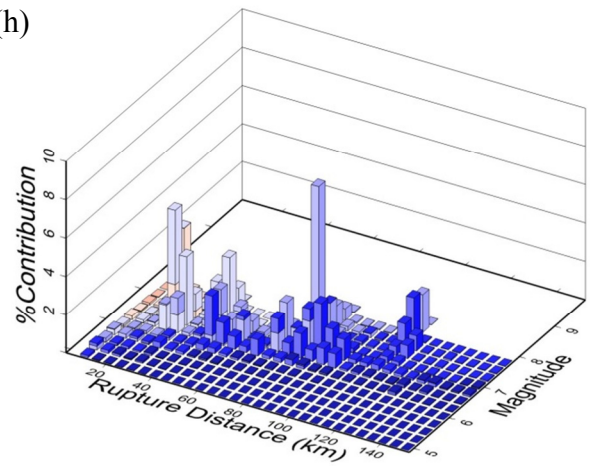

Case 8: Davis: SA(0.5s) for a 50% in 50 yrs hazard

(i)

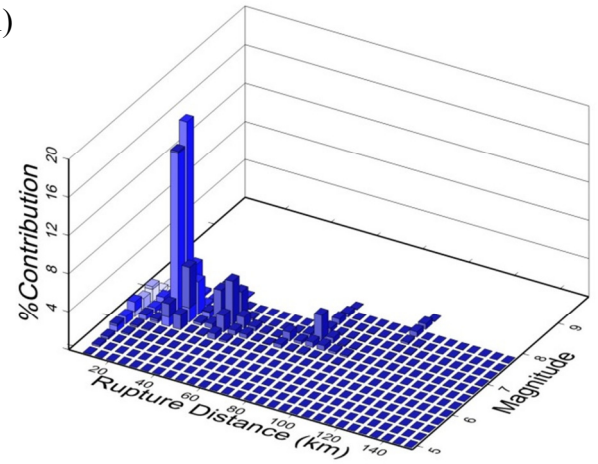

Case 9: Davis: SA(0.5s) for a 2% in 50 yrs hazard

(j)

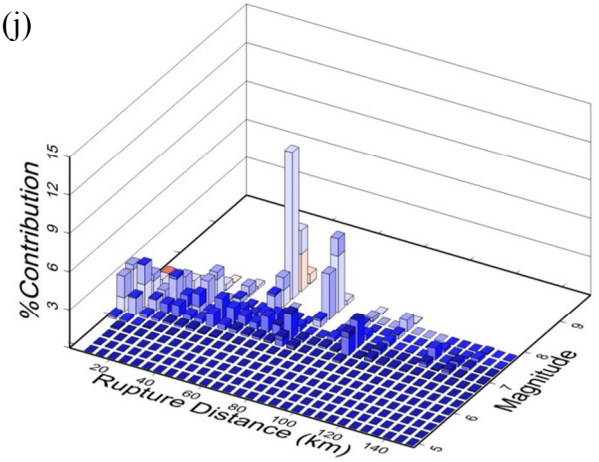

Case 10: Los Angeles: SA(3.0s) for a 50% in 50 yrs hazard

(k)

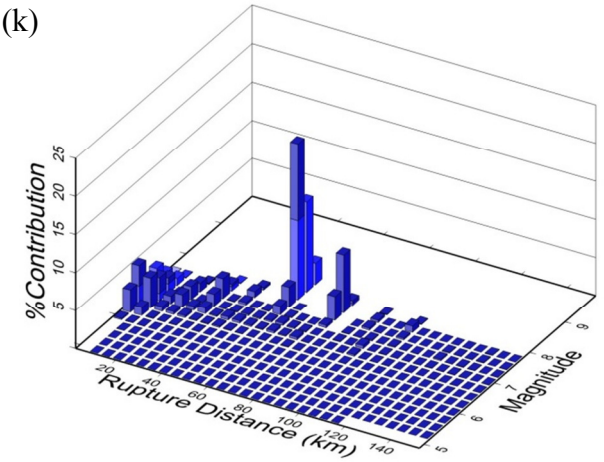

Case 11: Los Angeles: SA(3.0s) for a 2% in 50 yrs hazard

(l)

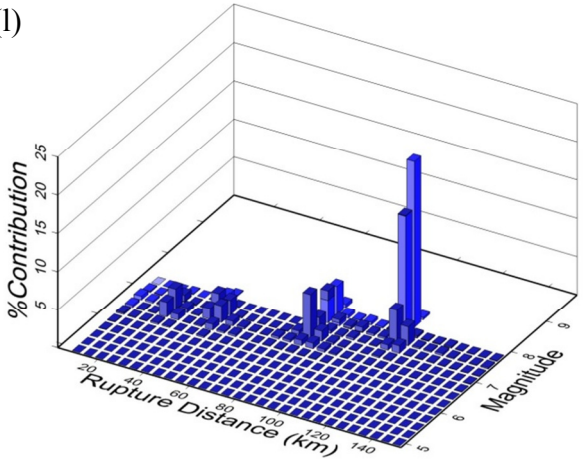

Case 12: Davis: SA(3.0s) for a 2% in 50 yrs hazard

Figure 12: (*Continued*): Deaggregation distribution of the 12 PSHA cases with the Vs30=200 m/s site condition: (g) Sacramento, SA (0.5s) hazard for a 2% in 50 years; (h) Davis, SA (0.5s) hazard for a 50% in 50 years; (i) Davis, SA (0.5s) hazard for a 2% in 50 years; (j) Los Angeles, SA (3.0s) hazard for a 50% in 50 years; (k) Los Angeles, SA(3.0s) hazard for a 2% in 50 years; (l) Davis, SA (3.0s) hazard for a 2% in 50 years.

3.2 Bounds considered on the implicit causal parameters

In this section, various bounding criteria for the magnitude and source-to-site distance of prospective ground motions are defined and applied to the considered deaggregation cases (presented in Table 11). These bounding criteria are compared in terms of their inclusiveness to encompass the M_w and R_{rup} distributions of the contributing scenarios and the so-called 'discounted' deaggregation contribution. The number of available ground motions based on the defined bounding criteria is also compared for the considered PSHA cases.

3.2.1 Definition of various bounding criteria

Since the seismic hazard from PSHA is contributed by several rupture scenarios, bounds on magnitude and source-to-site distance of prospective ground motions should be based on the distribution of these causal parameters obtained from deaggregation results. As a result, the determination of causal parameter bounds for M_w and R_{rup} in PSHA is significantly more complex than for scenario SHA (where there is a single target $M_w - R_{rup}$ combination). With the distributions of M_w and R_{rup} available from deaggregation, an obvious choice is to select bounds for each of these parameters based on certain percentiles. Also, similar to the scenario-based case (which is analogous to a deaggregarion case with a single contributing rupture scenario), it is also appropriate to allow for a certain range of causal parameters either side of the causal parameters for dominant contributing sources. Based on these two premises, bounding criteria presented in Table 12, denoted as criterion A, B, C, D, E, AC, and BD, are defined and examined for the considered deaggregation cases. These different criteria represent various perspectives on the trade-off between wider bounds with more inclusiveness of the deaggregation distribution, yet diminishing returns for the application of causal parameter bounds.

In order to clarify the definition of these criteria. Figure 13 schematically illustrates the definition of criteria A and C on the magnitude distribution of a sample deaggregation case. As illustrated in Table 12, for criterion A, the upper and lower bound limits of M_w and R_{rup} are set to values corresponding to 1st and 99th percentiles of their marginal distributions (from deaggregation results). For criterion B and E, these limits are set to values corresponding to 5th and 95th percentiles and 20th and 80th percentiles, respectively. For criterion C, the upper and lower limits are first set to values corresponding to 10th and 90th percentiles, and then further extended by a specified amount (as elaborated upon in the following paragraph). For magnitude and source-to-site distance, the specified amounts are $0.5M_w$ and $0.5R_{rup}$,

consistent with those proposed for the scenario-based ground motion selection in the earlier section of this report. Criterion D has a similar definition to criterion C, except the initial bound limits correspond to 20th and 80th percentiles.

Table 12: Bounding criteria examined on M_w and R_{rup} of prospective ground motions for PSHA-based ground motion selection

Criterion	Magnitude, M_w		Source-to-site distance, R_{rup}	
	Lower limit	Upper limit	Lower limit	Upper limit
A	$M_w^{1\%}$	$M_w^{99\%}$	$R_{rup}^{1\%}$	$R_{rup}^{99\%}$
B	$M_w^{5\%}$	$M_w^{95\%}$	$R_{rup}^{5\%}$	$R_{rup}^{95\%}$
C	$M_w^{10\%} - 0.5$	$M_w^{90\%} + 0.5$	$0.5R_{rup}^{10\%}$	$1.5R_{rup}^{90\%}$
D	$M_w^{20\%} - 0.5$	$M_w^{80\%} + 0.5$	$0.5R_{rup}^{20\%}$	$1.5R_{rup}^{80\%}$
E	$M_w^{20\%}$	$M_w^{80\%}$	$R_{rup}^{20\%}$	$R_{rup}^{80\%}$
AC	$min(M_w^{1\%}, M_w^{10\%} - 0.5)$	$max(M_w^{99\%}, M_w^{90\%} + 0.5)$	$min(R_{rup}^{1\%}, 0.5R_{rup}^{10\%})$	$max(R_{rup}^{99\%}, 1.5R_{rup}^{90\%})$
BD	$min(M_w^{5\%}, M_w^{20\%} - 0.5)$	$max(M_w^{95\%}, M_w^{80\%} + 0.5)$	$min(R_{rup}^{5\%}, 0.5R_{rup}^{20\%})$	$max(R_{rup}^{95\%}, 1.5R_{rup}^{80\%})$

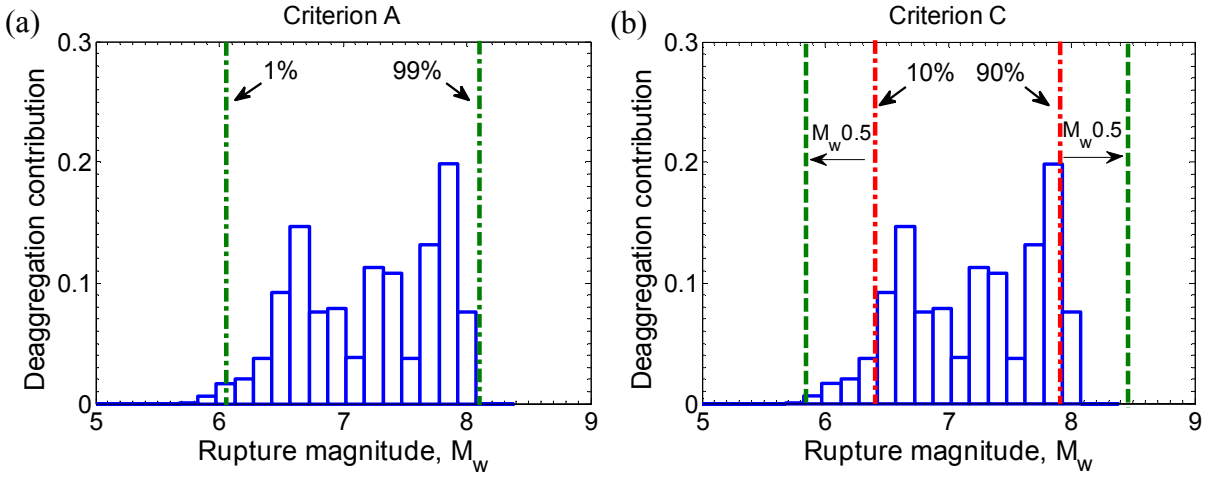

Figure 13: Schematic illustration of causal parameter bound criteria for M_w: (a) criterion A; (b) criterion C.

As shown in Figure 13, by using criterion A (or B and E), the scenarios within the bounds encompass most of the total contribution from the deaggregation results. However, for some deaggregation cases, scenarios with a large contribution can exist at tails of the distribution. For such cases, as-recorded ground motions with causal parameters in the vicinity of these scenarios, but beyond the limits, can still be relevant for ground motion selection. For instance, as shown in Figure 13a-b, the magnitude limits at 99% and 90% percentiles are equal to M_w8.1 and M_w7.8, respectively. It may be reasonable to assume that ground motions from ruptures up to M_w8.5 can still be relevant to represent intensity

measures of such scenarios. Therefore, setting bounds firmly to limits corresponding to certain percentiles might not result in reasonably wide bounds for ground motion selection. In this regard, similar to the approach taken for scenario-based ground motion selection where bounds are specified either side of the target scenario, bounds for PSHA-based ground motion selection can also be set in a similar manner to include ground motions with similar characteristics in the prospective ground motion subset. Criteria C and D are defined based on this approach, as presented in Table 12. Along this line, criteria A and C are combined in order to reach to wider causal parameter bounds. This criterion is denoted as AC, as presented in Table 12. Also, in order to obtain a moderately wide bound based on criteria B and D, these criteria were combined to a single criteria, denoted as BD (see Table 12). Finally, in order to investigate the effect of using narrow bounds on characteristics of selected ground motions, criterion E is defined based on limits corresponding to 20^{th} and 80^{th} percentiles of the M_w and R_{rup} distributions. Criterion E is aimed to only encompass scenarios with the largest contribution to the hazard for all types of deaggregation distributions considered.

3.2.2 Comparison of results from the different bounding criteria

Figure 14 presents the rupture magnitude distribution of the 12 deaggregation cases for the V_{s30}=200 m/s site condition, along with the magnitude bound limits determined based on the defined seven bounding criteria in Table 12. It can be seen that, for deaggregation cases with dominant scenarios at the tails of the distribution (i.e., cases 1 and 10-12); criteria A, B, and E result in relatively narrow bounds for which the limits are close to the scenarios with large contribution at the tail of the distribution. In contrast, criteria C and AC result in relatively wide bounds. The remaining criteria (i.e., D and BD) result in ranges similar to, but less than C and AC.

For deaggregation cases where the dominant scenarios occur near the centre of the magnitude distribution (i.e., cases 2-9), bound criteria B, D, E, and BD result in neglecting scenarios with small contributions at the tails of the distribution, which summed together can contribute significantly to the total hazard. In contrast, criterion A results in wider bounds that encompass the whole range of causal rupture scenarios. By using criteria AC, in comparison to criterion A, the defined bounds for these deaggregation cases become wider at one end (i.e., cases 2-5) or do not change (i.e., cases 6-9). From these considerations, criterion AC emerges as the widest criterion to apply bounds on magnitude, while criterion E results in the narrowest bound among the considered criteria. By using criterion E, in

particular, only ground motions with similar characteristics to the dominant scenario will be considered for ground motion selection, which can excessively restrict the number of available ground motions, and lead to poor ground motion selection results.

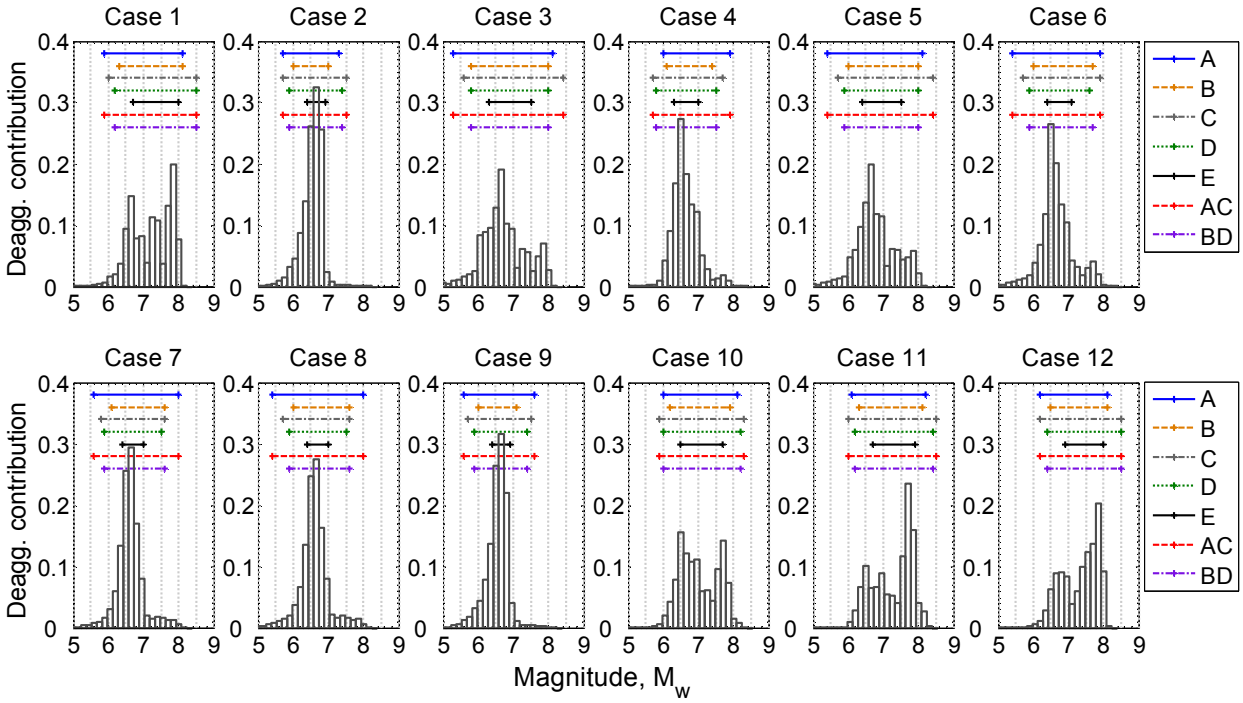

Figure 14: Application of causal parameter bounding criteria A, B, C, D, E, AC, and BD on magnitude distribution of deaggregation cases for V_{s30}=200 m/s site condition.

Figure 15 presents the source-to-site distance distribution of the 12 deaggregation cases for the V_{s30}=200m/s site condition, along with the R_{rup} bound limits determined based on the considered seven criteria presented in Table 12. It can be seen in Figure 15 that criteria B, D, E, and BD result in the most exclusion of scenarios at the tails of the R_{rup} distribution, whereas criteria A, C, and AC result in a relatively wide bounds that encompass the major contributing scenarios. Similar to rupture magnitude distributions, criterion E sets the bound limits close to the dominant scenarios, which results in neglecting other scenarios that in summation may contribute significantly to the hazard. Although not shown directly for brevity, the trends in Figure 14 and Figure 15 hold true for the V_{s30}=400 and 800 m/s site conditions as well.

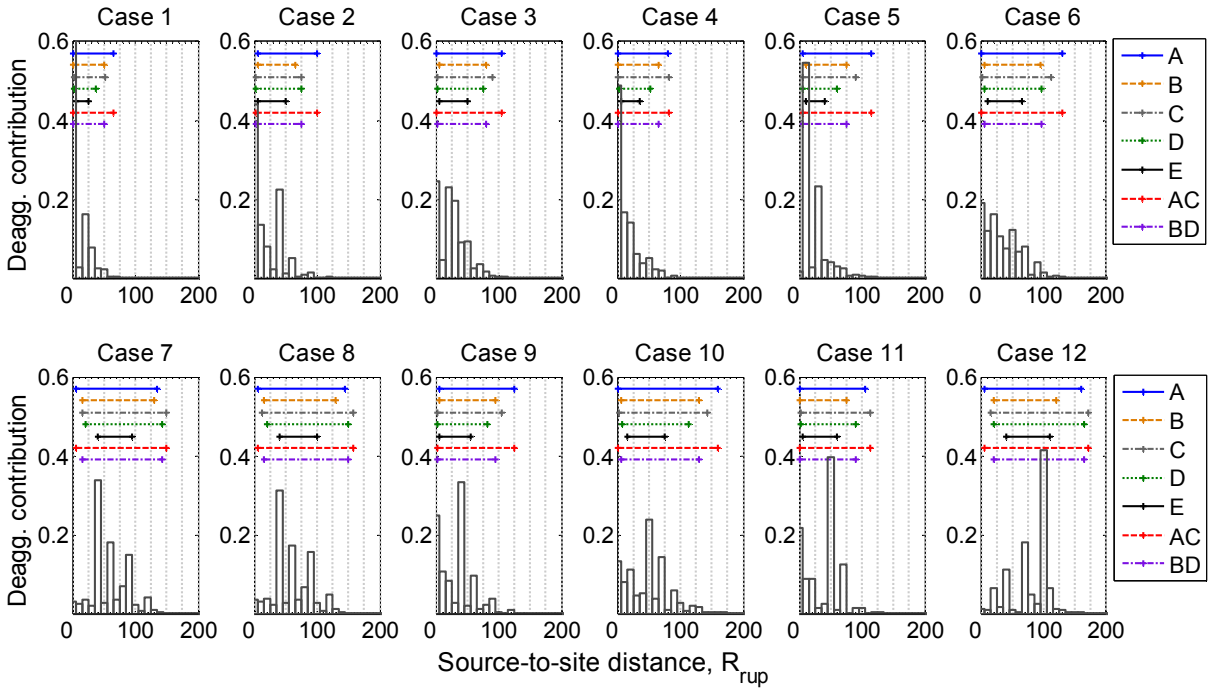

Figure 15: Application of causal parameter bounding criteria A, B, C, D, E, AC, and BD on source-to-site distance distribution of deaggregation cases for V_{s30}=200 m/s site condition.

In addition to the marginal distributions discussed in relation to Figure 14 and Figure 15, the considered bounding criteria are compared based on two other important factors, namely: (i) the deaggregation contribution that is 'discounted' (i.e., neglected) by applying bounds on magnitude and source-to-site distance of contributing scenarios; and (ii) the number of available ground motions in the database after applying bounds on the causal parameters. As an example among the three considered site conditions, Figure 16 presents the discounted deaggregation contribution versus the number of available ground motions in the NGA-West1 database (Chiou et al. 2008) for PSHA cases with the V_{s30}=200 m/s site condition. Figure 16 illustrates that wide bounds, such as criteria A and AC, result in the lowest discounted deaggregation contribution among the considered criteria for all of the deaggregation cases. This statement also holds true for the other site conditions considered in this study. In contrast, bounds such as B, D, and BD result in the largest discounted deaggregation contribution for all of the cases considered. It is noted that criterion E results in the lowest number of available ground motions and the largest discounted contribution in order of 0.5, which is out of the range for the presented results in Figure 16.

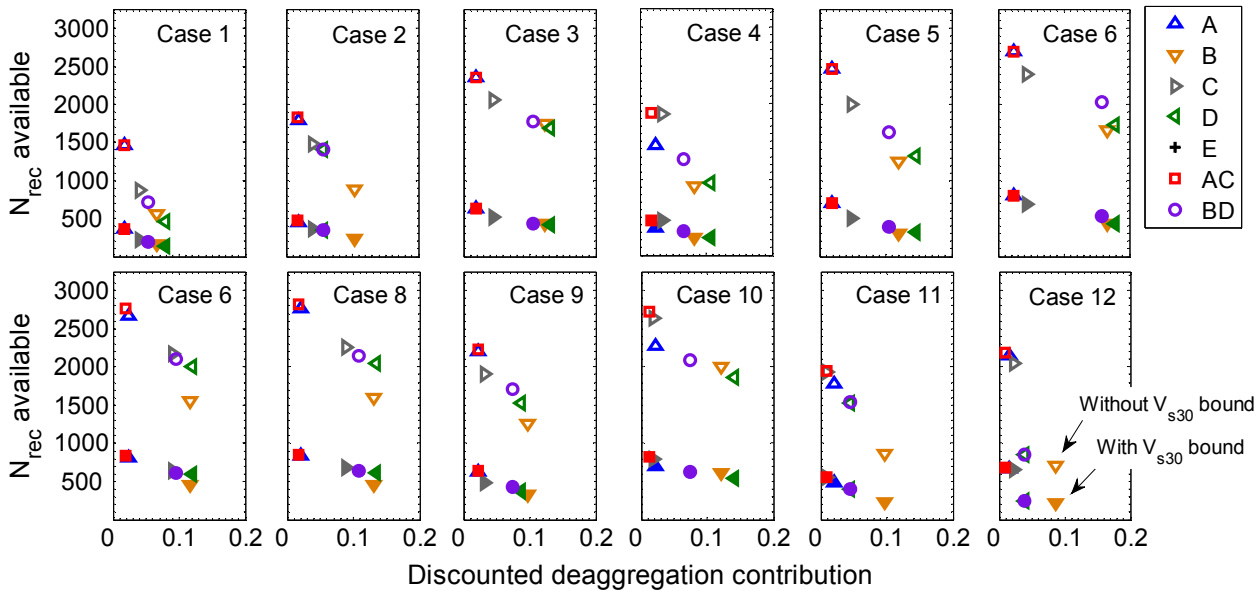

Figure 16: 'Discounted' deaggregation contribution versus the number of available ground motions for the 12 deaggregation cases with V_{s30}=200 m/s site condition. Open symbols illustrate the results based on only M_w and R_{rup} bounding criteria and the closed symbols illustrate the results based on the V_{s30} bound in addition to the M_w and R_{rup} bounds.

In order to investigate the effect of applying bounds on site condition of the prospective ground motions (i.e., V_{s30} bounds), the number of the available ground motions for each PSHA case is calculated twice; first based on M_w and R_{rup} bounds only, and then based on bounds on the site condition (i.e., V_{s30} bound) in addition to the M_w and R_{rup} bounds. The considered bounds on V_{s30} values of prospective ground motions are the same as those considered for the scenario-based ground motion selection as noted in Table 3. As shown in Figure 16, the number of available ground motions based on the A and AC criteria are the largest among the considered criteria. This is obviously because of the wide M_w and R_{rup} bounds considered by these criteria. As shown, the number of the available ground motions after applying the V_{s30} bound decreases significantly for the V_{s30}=200 m/s site condition.

The number of available ground motions for the considered 36 PSHA cases are presented in Table 13 based on the AC criterion as the widest bound among the considered criteria in this study. As illustrated in Table 13, by applying bounds on the site condition, the number of the available ground motions decreases significantly for the V_{s30}= 200 and 800m/s site conditions, in contrast, the reduction for the V_{s30}=400m/s site condition is not large. This is due to a relative abundance in the number of ground motions in the NGA-West1 database (Chiou et al. 2008) recorded on stiff soil deposits in comparison to those recorded on soft soil or soft rock deposits. Considering the large reduction in the number of available ground

motions after application of the V_{s30} bounds, using a wide bounding criteria such as AC on M_w and R_{rup} ensures that the prospective ground motions databases is not overly restricted to a small number of available ground motions.

Table 13: Number of available ground motion records (N_{rec}) for the considered PSHA cases based on bound criterion AC on M_w and R_{rup}, and the V_{s30} bound

	Bounds only on M_w and R_{rup}			Bounds on M_w, R_{rup}, and V_{s30}		
Deagg. case	V_{s30}=200	V_{s30}=400	V_{s30}=800	V_{s30}=200	V_{s30}=400	V_{s30}=800
1	1463	1565	1821	355	1282	938
2	1835	1866	2662	467	1522	1303
3	2356	2356	2356	633	1901	1187
4	1868	1695	1850	459	1386	946
5	2467	2768	2467	703	2233	1219
6	2692	2692	2692	802	2163	1311
7	2765	2772	2815	838	2231	1354
8	2815	2913	2805	854	2349	1340
9	2227	2750	2772	639	2212	1338
10	2728	2728	2728	830	2181	1334
11	1944	2563	2652	557	2049	1307
12	2181	2669	2752	681	2138	1338

In order to compare the widest and narrowest bounding criteria considered in this study (i.e., criterion AC and E, respectively) in terms of the number of prospective ground motions, Table 14 presents the number of available ground motions based on criterion E and the V_{s30} bound for the 36 PSHA cases considered. By comparing these values with those presented in Table 13 based on criterion AC, it is evident that using bounds that only encompass the scenarios with largest contribution to the hazard (i.e., criterion E) will significantly reduce the number of available ground motions. It is important to note that a balance should exist between using excessively wide bounds which provide no meaningful benefit (i.e. no different in comparison to having no bounds at all) and using excessively narrow bounds which result in too few prospective ground motions. As previously mentioned, implicit causal parameters are considered of secondary importance relative to explicit IMs to characterize the intensity of ground motions for the purpose of ground motion selection. Therefore, using excessively narrow causal parameter bounds seems unnecessary, and as shown in the subsequent section, it can be detrimental from a view point that the remaining ground motions might not be able to appropriately represent the distribution of explicit IMs for the target hazard.

Table 14: Number of available ground motion records (N_{rec}) for the considered PSHA cases based on bound criterion E on M_w and R_{rup}, and bound on V_{s30}

	Bounds only on M_w and R_{rup}			Bounds on M_w, R_{rup}, and V_{s30}		
Deagg. case	V_{s30}=200	V_{s30}=400	V_{s30}=800	V_{s30}=200	V_{s30}=400	V_{s30}=800
1	126	126	248	31	103	125
2	178	178	195	53	145	69
3	394	394	394	115	327	165
4	221	126	283	73	103	127
5	191	366	191	56	306	71
6	271	271	271	78	225	103
7	171	157	182	38	132	72
8	182	160	398	42	134	184
9	193	229	165	55	197	68
10	499	499	499	129	396	233
11	346	462	474	83	372	230
12	393	474	311	123	376	112

Based on the presented results in this section, criteria AC is advocated as a suitable causal parameter bounding criterion to account for the full distribution of causal rupture scenarios and consider an extension beyond the dominant scenarios at the tails of the deaggregation distribution, and is adopted in the presented results to follow. While this criterion is recommended to be used as an initial bounding criterion for general PSHA cases, it is important to note that the user judgement should be utilized in defining the bounding criterion for a specific problem in order to incorporate the characteristics of the problem at hand.

3.3 Characteristics of the selected ground motion ensembles

In order to understand the overall impact of using causal parameter bounds, this section compares the IM distributions of selected ground motions with respect to the corresponding target GCIM distributions for the considered PSHA cases. A total of 20 ground motions are selected, using 10 replicate selections (Bradley 2012c, Tarbali and Bradley 2014b), for each of the 36 PSHA-based cases considered. Three types of causal parameter bounds are considered: no bounds, narrow bounds (i.e., criterion E and the V_{s30} bound), and wide bounds (i.e., criterion AC and the V_{s30} bound). In order to first illustrate shortcomings in common ground motion selection approaches in which the selection is based only on SA ordinates, ensembles of ground motions are firstly selected by considering only SA ordinates in the weight vector (i.e., the 'SA only' weight vector in Table 6). It is noted that for PSHA-based ground motion selection based on no causal parameter bounds, Bradley (2012c) has

previously demonstrated bias in distribution of IMs other than SA ordinates when the selection process is based on only SA ordinates. Thus, the aim here is to investigate whether or not considering bounds on the causal parameters can strictly account for the effect of neglecting important IMs that characterize different aspects of ground motions. Subsequently, the effect of considering bounds on the causal parameters is examined when multiple IM types (i.e., SA ordinates, duration, and cumulative effects) are considered via the 'generic' weight vector presented in Table 6.

3.3.1 Explicit intensity measures of selected ground motions—selection based on only SA ordinates

Figure 17 presents the acceleration spectra of ground motions selected based only on SA ordinates (i.e., weight vector 'SA only' in Table 6) and their corresponding median, 16th, and 84th percentiles representing the target SA distribution for a sample PSHA case (i.e., case 7) with the V_{s30}=200 m/s site condition. As illustrated in Figure 17a-b, ground motions selected 'without bounds' and with 'wide bounds' (i.e. criterion AC) on the causal parameters have an appropriate representation of the target SA distribution by having the median, 16th, and 84th percentiles of the selected ground motions close to the target GCIM distribution. Figure 17c illustrates, in contrast, that considering 'narrow bounds' (i.e. criterion E) on the causal parameters results in selected ground motions with a poor representation of the target SA distribution due to removing an excessive number of ground motions from the database that can appropriately represent the target hazard. Bias in the distribution of SA ordinates when narrow bounds are applied is present for most of the 36 PSHA cases and site conditions considered. As presented in Table 13 and Table 14, the number of available ground motions based on the narrow bounds for the PSHA case considered in Figure 17 (i.e., case 7) is 38, whereas, by using wide bounds the number of available motions is 838. Based on the obtained results for the other cases considered, it is noted that the large difference between the number of available ground motions based on narrow and wide bounds is an indicative of a possible degradation in representation of the ground motions selected based on narrow bounds.

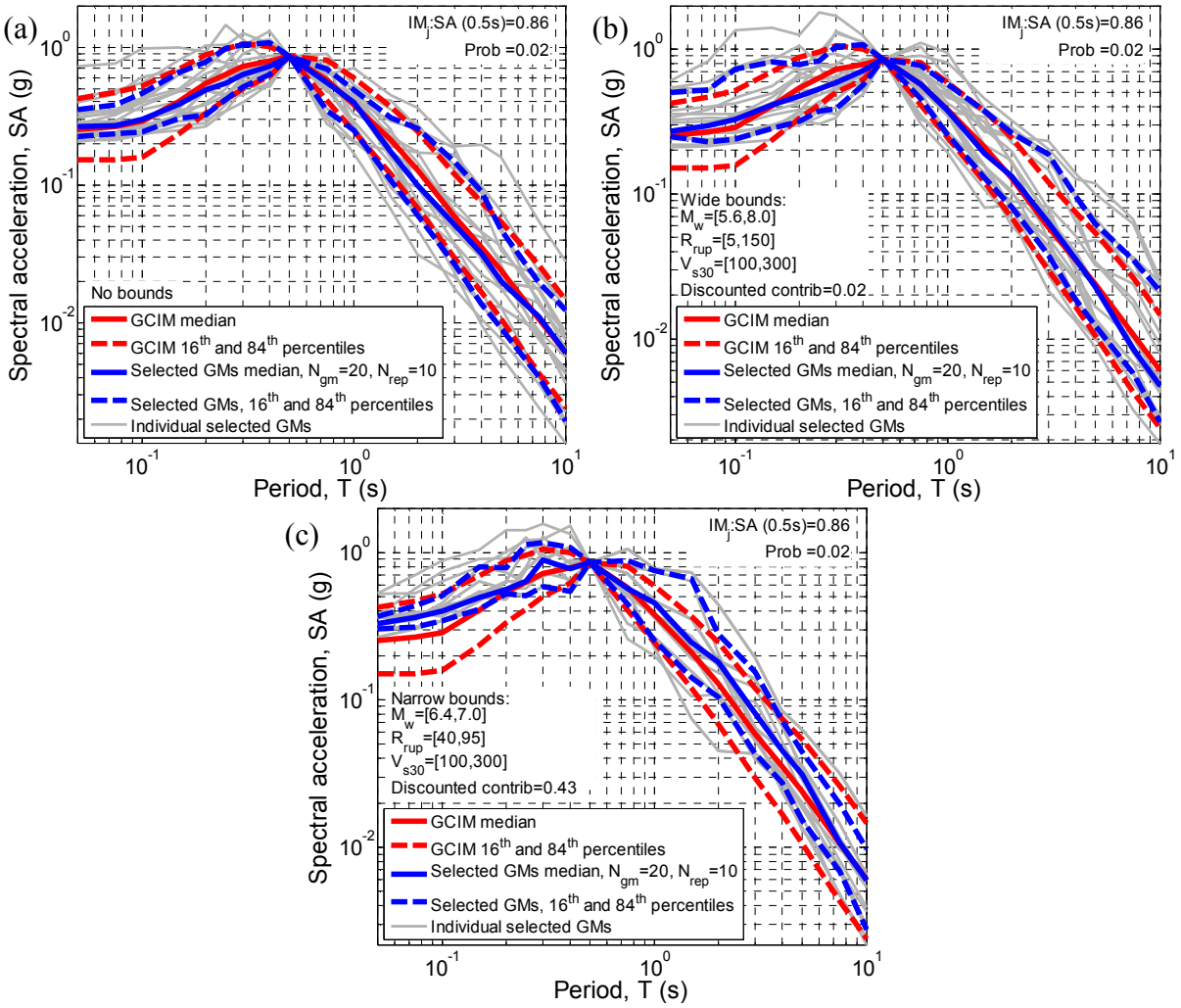

Figure 17: Acceleration spectra of selected ground motions by considering only SA ordinates in the weight vector for a sample PSHA case (i.e., case 7 with V_{s30}=200 m/s site condition) and the corresponding median, 16th, and 84th percentiles for ensembles selected: (a) without bounds; (b) with wide bounds (criterion AC); (c) with narrow bounds (criterion E).

In order to investigate the distribution of IMs other than SA ordinates when ground motions are selected based on only SA ordinates, Figure 18 presents the CAV and D_{s575} distributions of the selected ground motions for various PSHA cases with the V_{s30}=200 m/s site condition. While the use of no bounds or wide bounds enabled a good representation of the SA distributions, as shown in Figure 18, neither option explicitly addresses the bias in the distribution of these IMs representing cumulative and duration-related aspects of ground motions. This issue was also observed in the previous section for scenario-based ground motion selection (i.e., Figure 2).

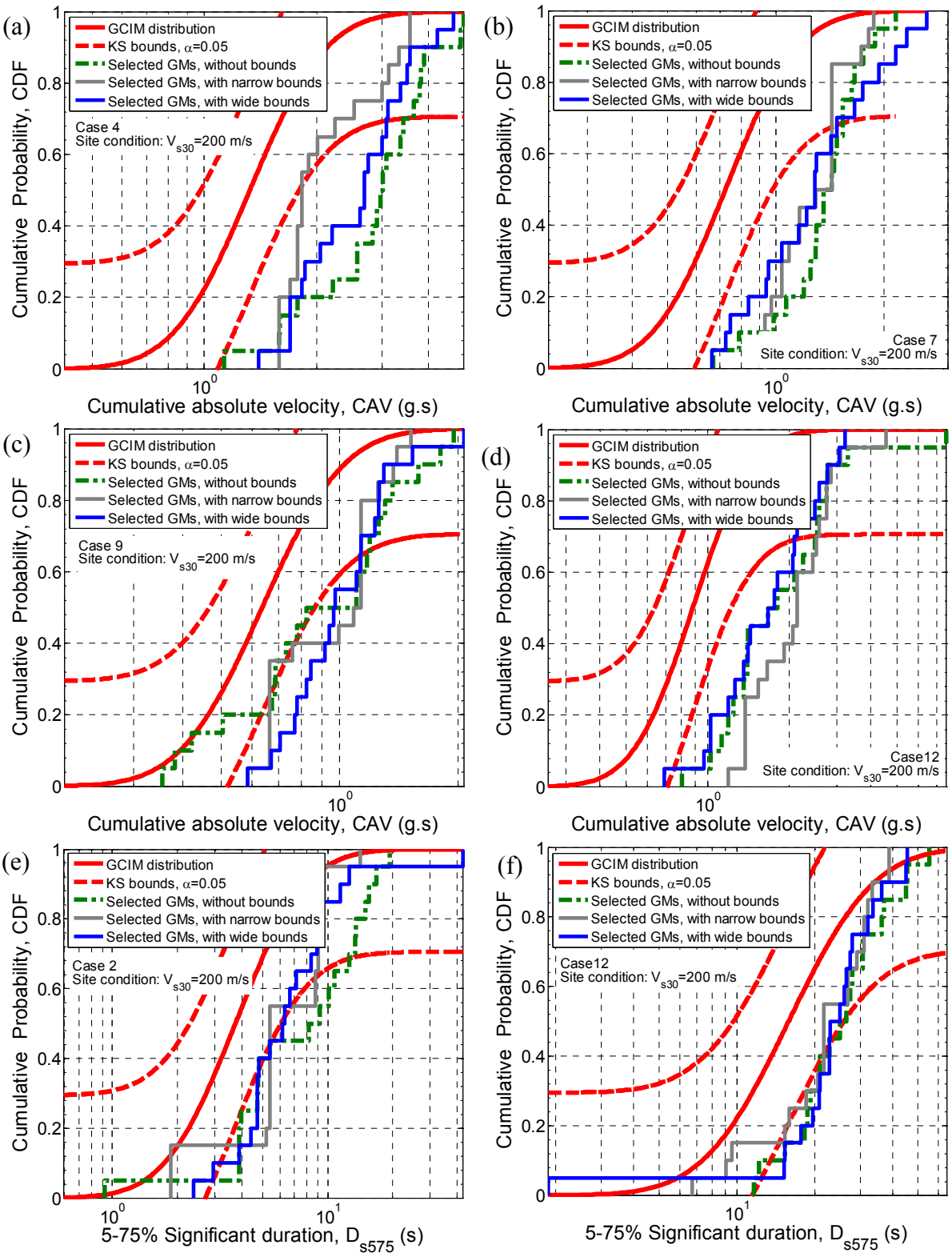

Figure 18: Properties of selected ground motions by considering only SA ordinates in the weight vector for sample PSHA cases with V_{s30}=200 m/s site condition based on wide (criterion AC) and narrow (criterion E) causal parameter bounds and also without bounds: (a)-(d) distribution of CAV; (e)-(f) distribution of D_{s575}.

Similar to the results presented in Figure 18, Figure 19 presents the CAV and D_{s575} distributions of the selected ground motions based on only SA ordinates for sample PSHA cases with V_{s30}=400 and 800 m/s site conditions. As shown in Figure 19, considering (narrow or wide) bounds on the causal parameters does not result in remediating the bias in distribution of IMs that are not considered in the weight vector as was the case for the V_{s30}=200 m/s cases in Figure 18. Although not presented here for brevity, selection based on narrow bounds also results in a biased distribution of SA ordinates for most of the PSHA cases with V_{s30}=400 and 800 m/s site conditions considered.

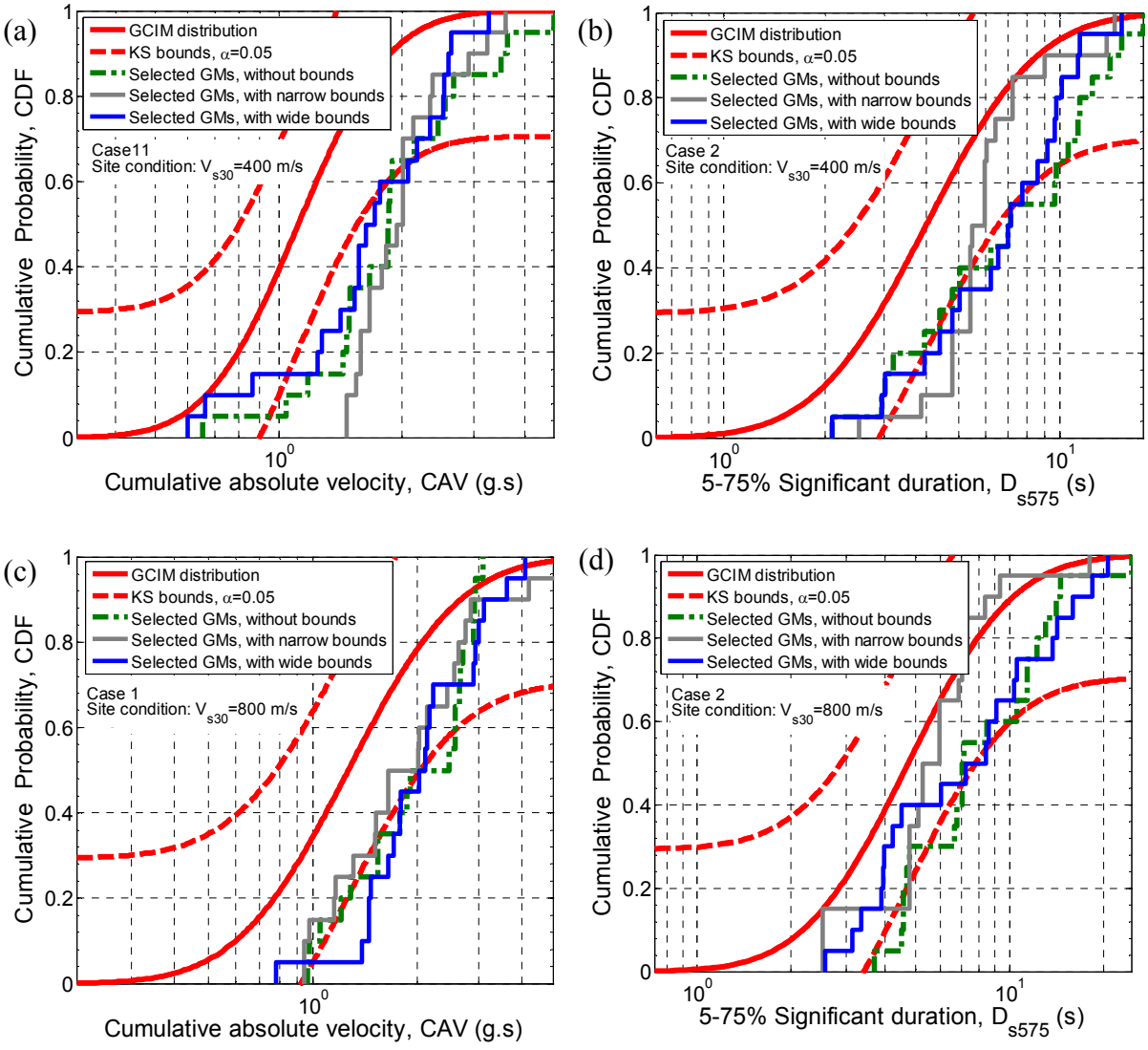

Figure 19: Properties of selected ground motions by considering only SA ordinates in the weight vector for sample PSHA cases with V_{s30}=400 and 800 m/s site conditions based on wide (criterion AC) and narrow (criterion E) causal parameter bounds and also without bounds: (a)-(d) distribution of CAV; (e)-(f) distribution of D_{s575}.

It should be noted that the conventional purpose of applying bounds on the causal parameters when the selection is based on only SA ordinates is to attain an appropriate representation for IMs other than SA ordinates that are not considered in the weight vector. This is based on an assumption that the causal parameter bound does not degrade the quality of selected ground motions in representing the target SA distribution. However, as shown in Figure 17 for a sample PSHA case among others, using narrow bounds can violate this assumption, resulting in a poor representation for the SA ordinates themselves. In addition, it is demonstrated in Figure 18 and Figure 19 that using causal parameter bounds (either narrow or wide) is not a reliable approach to strictly account for duration and cumulative effects of ground motions when ground motion selection is based on only SA ordinates.

3.3.2 Explicit intensity measures of selected ground motions—selection based on SA, duration, and cumulative effects

As discussed by Bradley (2012c) and Tarbali and Bradley (2014b), bias in the distribution of IMs other than SA ordinates when selecting ground motions can be resolved by explicitly considering them in the weight vector. In order to address this issue, ground motions are selected based on the generic weight vector presented in Table 6, which incorporates ground motion amplitude, frequency content, duration, and cumulative effects. Figure 20 presents the acceleration spectra of ground motions selected based on the generic weight vector and their corresponding median, 16th, and 84th percentiles representing the target SA distribution for PSHA case 7 with V_{s30}=200 m/s. Ground motions selected for this PSHA case based on only SA ordinates were previously illustrated in Figure 17. Figure 20a-c compares the representation of the selected ground motions using the generic weight vector based on no bounds (Figure 20a), wide bounds (Figure 20b), and narrow bounds (Figure 20c). It can be seen that considering narrow bounds has a detrimental effect on representativeness of the selected ground motions to the target SA distribution, while, considering wide bounds or no bounds does not have such negative effects. Although not presented here for brevity, this holds true for all of the PSHA cases and site conditions considered in this study. This is due to the fact that, as mentioned previously for ground motions selected based on only SA ordinates (i.e., Figure 17), using narrow causal parameter bounds removes an excessive number of ground motions which can appropriately represent the target distribution of IMs, whereas, the wide bounds does not have such detrimental effects.

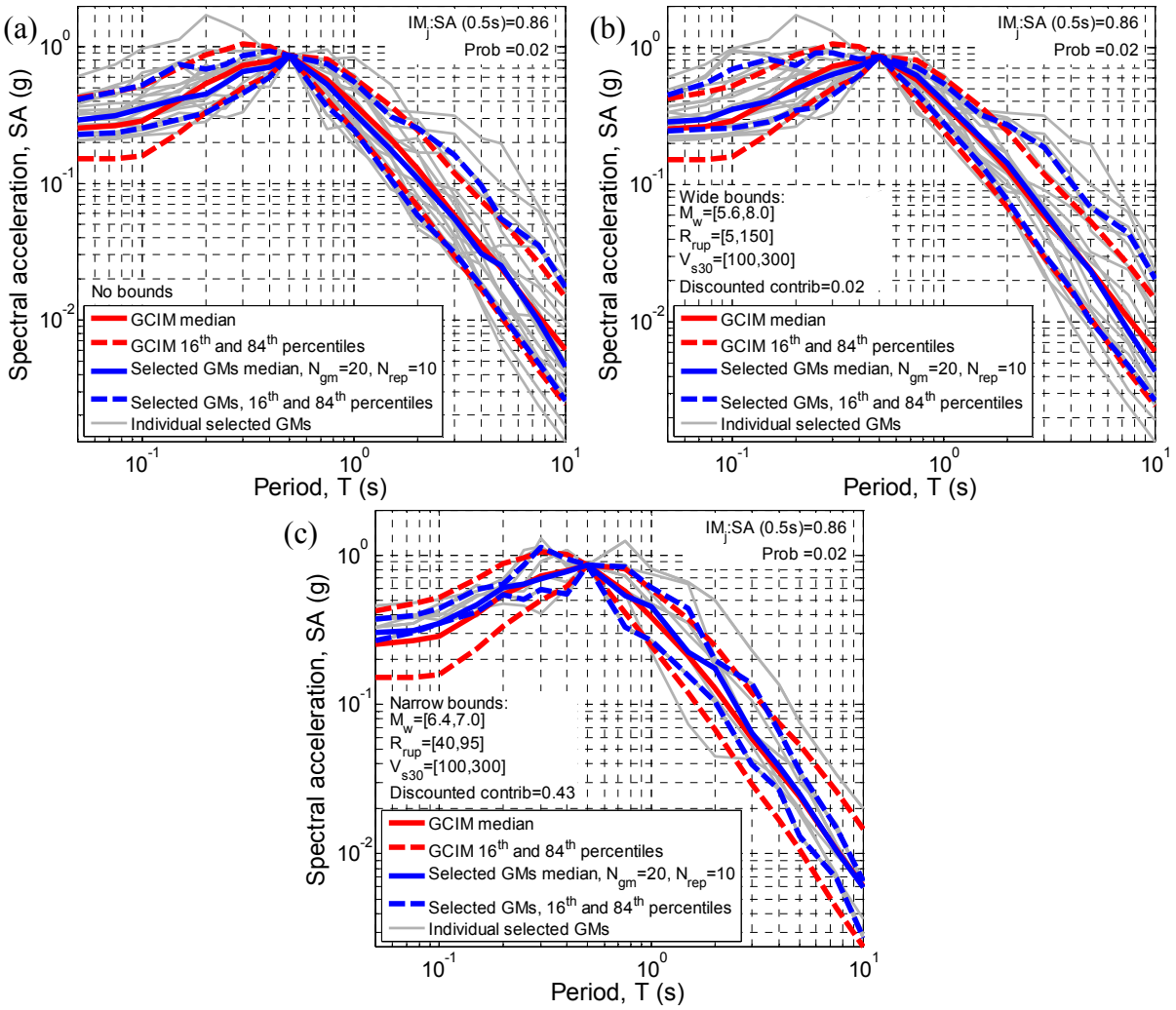

Figure 20: Acceleration spectra of selected ground motions based on the generic weight vector (i.e., including SA, duration, and cumulative IMs) for a sample PSHA case (i.e., case 7 with V_{s30}=200 m/s site condition) and their median, 16th, and 84th percentiles for ensembles selected: (a) without bounds; (b) with wide bounds (criterion AC); (c) with narrow bounds (criterion E).

In order to examine characteristics of the IMs other than SA ordinates when ground motions are selected based on the generic weight vector, the CAV and D_{s575} distributions of the selected ground motions for the same PHSA cases presented in Figure 18 (that were selected based on only SA ordinates) are shown in Figure 21. It can be seen that by using an appropriate weight vector (i.e., considering amplitude, frequency content, duration, and cumulative effects), bias in distribution of ground motions selected without bounds is completely removed, or for some cases significantly improved (e.g., Figure 21b and Figure 21d). In addition, Figure 21 illustrates that ground motions selected based on wide bounds have an appropriate representation of the target distribution, whereas using narrow bounds can result in a biased distribution for some PSHA cases.

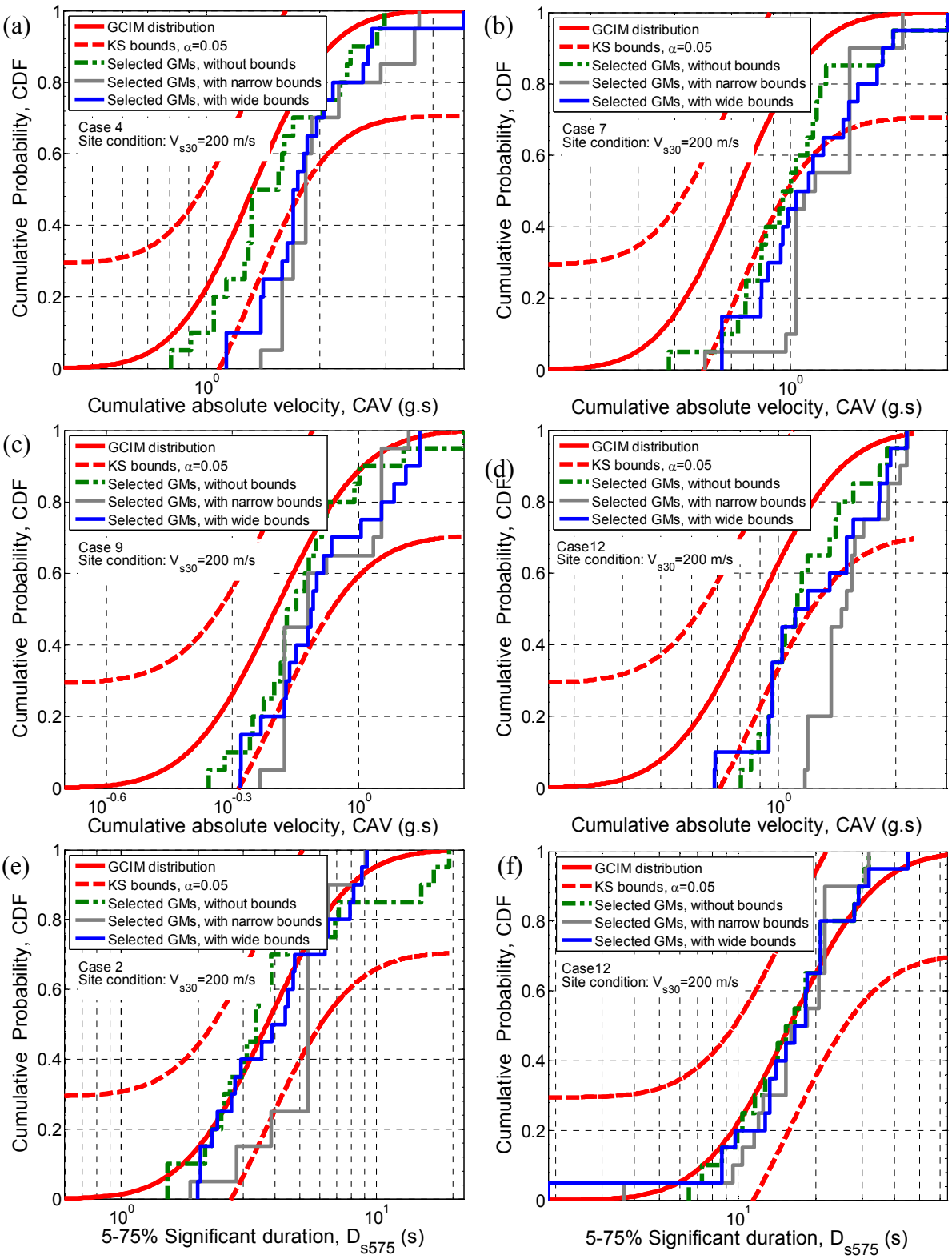

Figure 21: Properties of selected ground motions for the same sample PSHA cases presented in Figure 18 with V_{s30}=200 m/s site condition, by considering amplitude, frequency content, duration, and cumulative effect in the weight vector (i.e., generic weight vector in Table 6) using wide (criterion AC) and narrow (criterion E) causal parameter bounds and also without bounds: (a)-(d) distribution of CAV; (e)-(f) distribution of D_{s575}.

The reason for still having bias (for selected ground motions without bounds and with wide bounds) for the cases presented in Figure 21b and Figure 21d can be considered as a combination of the limited number of available ground motions for soft soil sites, and that ground motions recorded on soft soil sites are more complex to be simply characterized by limited number of IMs using only the V_{s30} parameter to characterize the site condition.

In order to investigate the distribution of IMs other than SA ordinates for PSHA cases with V_{s30}=400 and 800 m/s site conditions when the generic weight vector is implemented for selection, Figure 22 presents the CAV and D_{s575} distributions of the selected ground motions for the same sample PSHA cases presented in Figure 19 (for which the selection was based on only the SA ordinates). As presented in Figure 22, and by comparing with the results presented in Figure 19, it can be seen that the bias in distribution of IMs representing the duration and cumulative effects of ground motions selected for the V_{s30}=400 and 800 m/s site conditions is resolved for ground motions selected based on the generic weight vector. Also, ground motions selected based on wide bounds have an appropriate representation of the target distribution. However, ground motions selected based on narrow bounds might still have bias or a poor representation to the target distribution of IMs, as shown in Figure 22a and Figure 22c for sample PSHA cases.

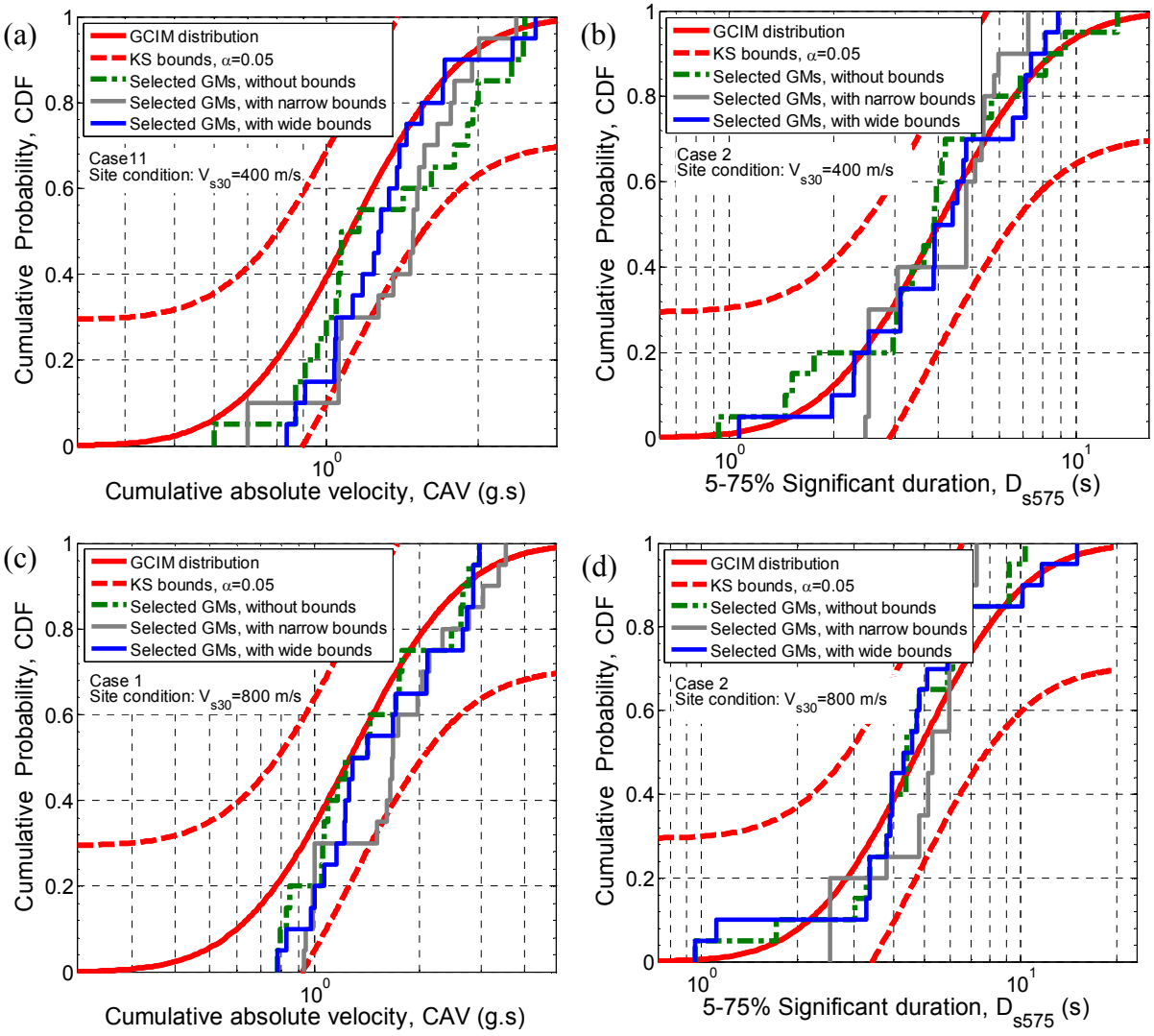

Figure 22: Properties of selected ground motions for the same sample PSHA cases presented in Figure 19 with V_{s30}=400 and 800 m/s site conditions, by considering amplitude, frequency content, duration, and cumulative effects in the weight vector (i.e., generic weight vector in Table 6) using wide (criterion AC) and narrow (criterion E) causal parameter bounds and also without bounds: (a)-(d) distribution of CAV; (c)-(d) distribution of D_{s575}.

3.3.3 Overall representation of selected ground motion ensembles for all PSHA cases considered

In order to obtain an overall view on the suitability of selected ground motion ensembles in comparison to the target IM distributions, Figure 23 presents the global misfit of the selected ground motion ensembles for all of the considered PSHA cases and site conditions. It is noted that the selected ground motions are based on the generic weight vector presented in Table 6, which includes weights on SA, duration, and cumulative effects. Figure 23a compares the global misfits for ensembles selected based on no bounds with those selected based on the narrow bounds (i.e., criterion E and V_{s30} bound), in which it can be seen

that the selected ensembles have larger global misfits for most of the PSHA cases if narrow bounds are utilized, which is most accentuated for V_{s30}=200 m/s site condition due to the small number of available ground motions after the narrow bounds are applied (see Table 14). The large bias in distribution of SA ordinates and other IMs presented in Figure 20 and Figure 21 illustrate the reasons for the large global misfits of ensembles selected based on narrow bounds. In contrast, ground motions selected based on wide bounds (i.e., criterion AC and V_{s30} bound), as presented in Figure 23b, result in global misfits that are almost equal to those selected based on no bounds.

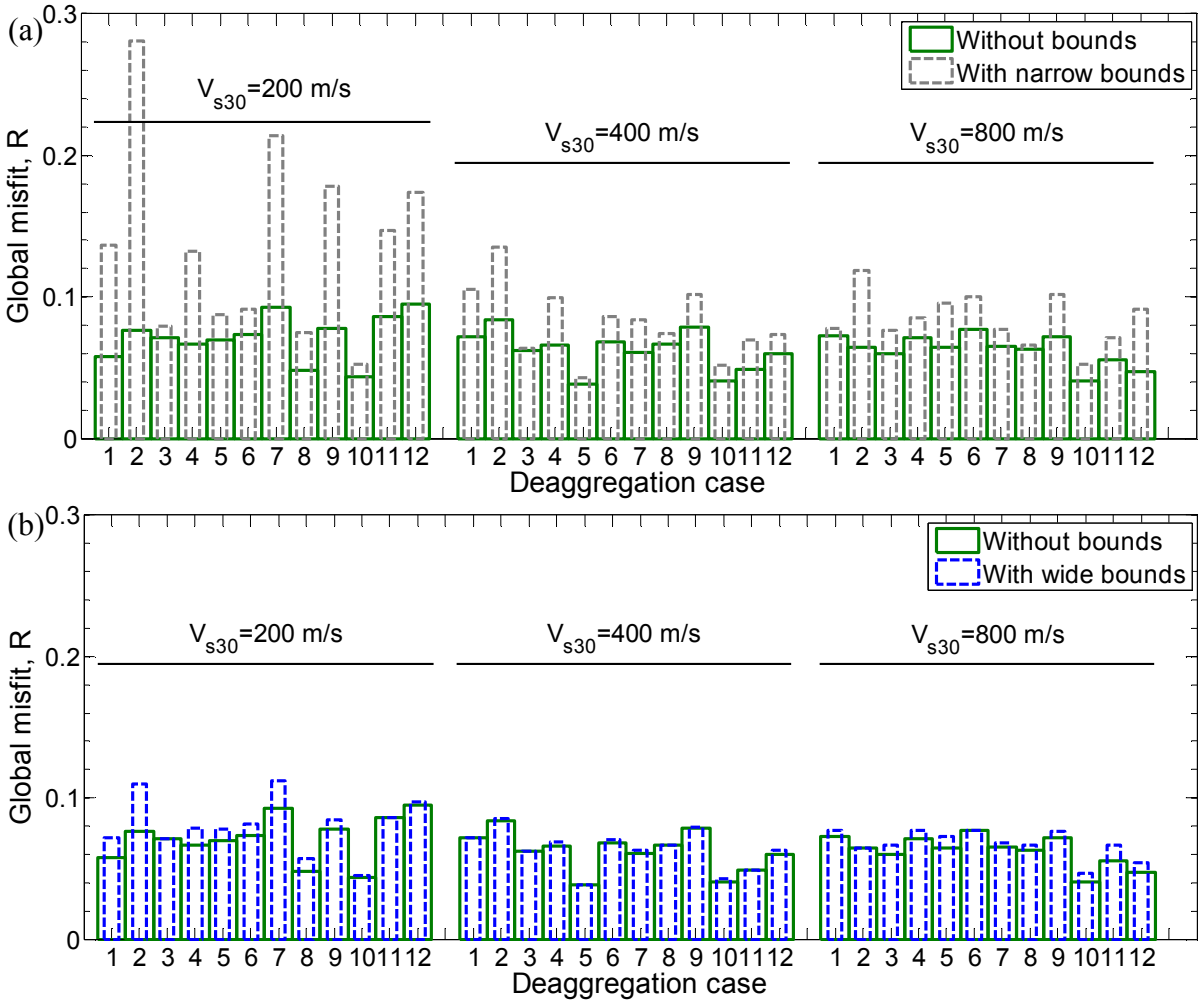

Figure 23: Global misfit of selected ground motion ensembles for all of the considered PSHA cases and site conditions: (a) comparison between ensembles selected based on no bounds with those selected based on narrow bounds; (b) comparison between ensembles selected based on no bounds with those selected based on wide bounds.

Based on the presented results for different PSHA cases and site conditions, it is demonstrated that using narrow bounds can unreasonably remove appropriate ground motions from the database and result in a biased distribution of IMs for some PSHA cases. Therefore,

it is recommended to use 'wide' M_w and R_{rup} bounds on prospective ground motions such as criterion AC implemented in this study. It is noted that this criterion sets the bounds in a way that most of the contributing scenarios from the deaggregation result are included in addition to extending the bound limits to accommodate ground motions with similar characteristics to any dominant scenario near the tail of the deaggregation distribution (see Figure 14 and Figure 15). In addition to considering wide bounds on M_w and R_{rup}, it is recommended to constrain the prospective ground motions to those recorded on sites with similar sub-surface soil condition. This can be achieved by constraining the V_{s30} of prospective ground motions as recommended in Table 3.

3.3.4 Implicit causal parameters of selected ground motions

In addition to the effect of causal parameter bounds on explicit IMs of ground motions, bounds consideration affects the causal parameter distribution of selected ground motions, as discussed in this section. Figure 24 and Figure 25 present the M_w and R_{rup} distributions, respectively, of the selected ground motions and the corresponding deaggregation distribution for 3 PSHA cases (i.e., cases 4, 6, 10) for the V_{s30}=400 m/s site condition. In all three depicted cases it can be seen that the use of narrow bounds results in ground motions with causal M_w and R_{rup} values closest to the deaggregation distributions, followed by the use of wide bounds, and then no bounds. However, it is noted that this close fit with the use of narrow causal parameter bounds comes with the aforementioned problem of ground motions having a poor fit to the target IM distributions. In contrast, it can be seen that the use of 'wide' bounds leads to a consistent improvement in the empirical distributions of the selected ground motions as compared to the marginal M_w and R_{rup} hazard deaggregation distributions, and ground motion ensembles which provide a good fit to the target IM distributions.

In particular, as shown in Figure 24a as an example for deaggregation cases with large magnitude causal scenarios in the near-fault region (i.e., cases 1-5), the causal magnitude of ground motions selected based on wide bounds has a close distribution to the deaggregation results which is almost within the KS test bound of the deaggregation distribution. In contrast, the magnitude distribution of ground motions selected based on no bounds does not have an appropriate representation of the target deaggregation distribution. Also, ground motions selected with narrow bounds do not represent the large variance in magnitude distribution of the causal scenarios, appropriately.

For deaggregation cases with a large variability in the M_w and R_{rup} of contributing causal scenarios (i.e., cases 6-8), Figure 24b illustrates that the selected ground motions based on narrow bounds have an appropriate representation of the median value of the deaggregation magnitude, however, with a poor representation of the variance of the distribution. Selected ground motions based on no bounds and wide bounds both result in similar distributions, with an appropriate representation of the deaggregation variance but larger median values. As shown in Figure 24c for deaggregation cases with dominant scenarios (i.e., cases 9-12), ground motions selected based on narrow bounds have a closer distribution to the target magnitude distribution, which is within the KS test bound.

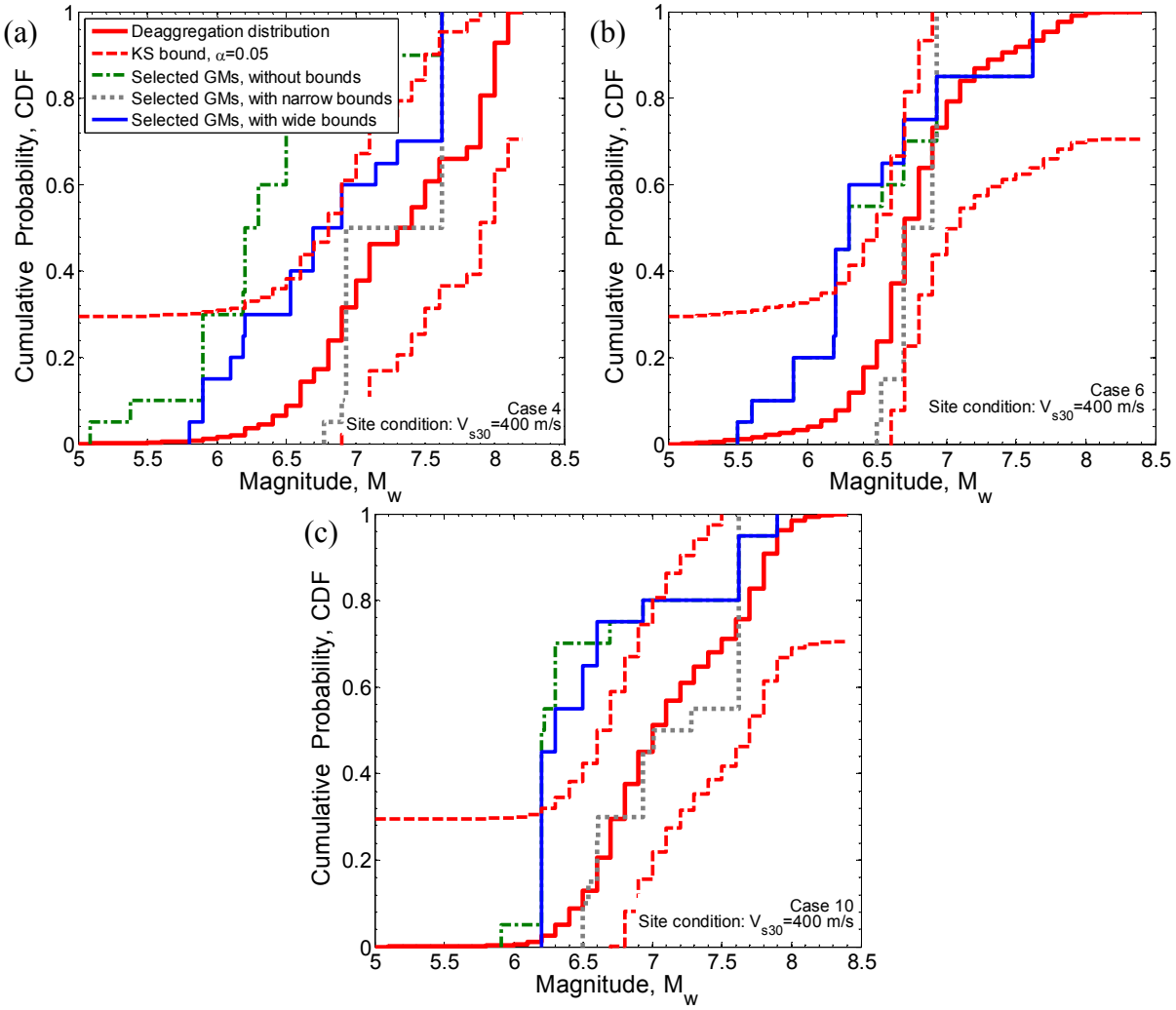

Figure 24: Comparison between magnitude distribution of selected ground motions and the deaggregation results for sample PSHA cases with V_{s30}=400 m/s site condition: (a) case 4; (b) case 6; (c) case 10.

Figure 25 compares the source-to-site distance distribution of selected ground motions and the corresponding deaggregation distributions for 3 PSHA cases (i.e., cases 4, 6, 10) for the V_{s30}=400 m/s site condition. As shown in Figure 25a, for deaggregation cases with causal

scenarios in the near-fault region, ground motions selected based on narrow bounds have R_{rup} values closer to the deaggregation results than the ensembles selected based on no bounds or wide bounds. In contrast, for deaggregation cases with R_{rup} values distributed in a large range (i.e., cases 6-8), or cases with dominant scenarios (i.e., cases 9-12), ground motions selected based on no bounds and wide bounds result in R_{rup} distributions similar to the deaggregation results, which are within the KS test bound (see Figure 25b-c). The R_{rup} distributions of the ensembles selected based on narrow bounds can slightly deviate from the KS test bounds for these cases.

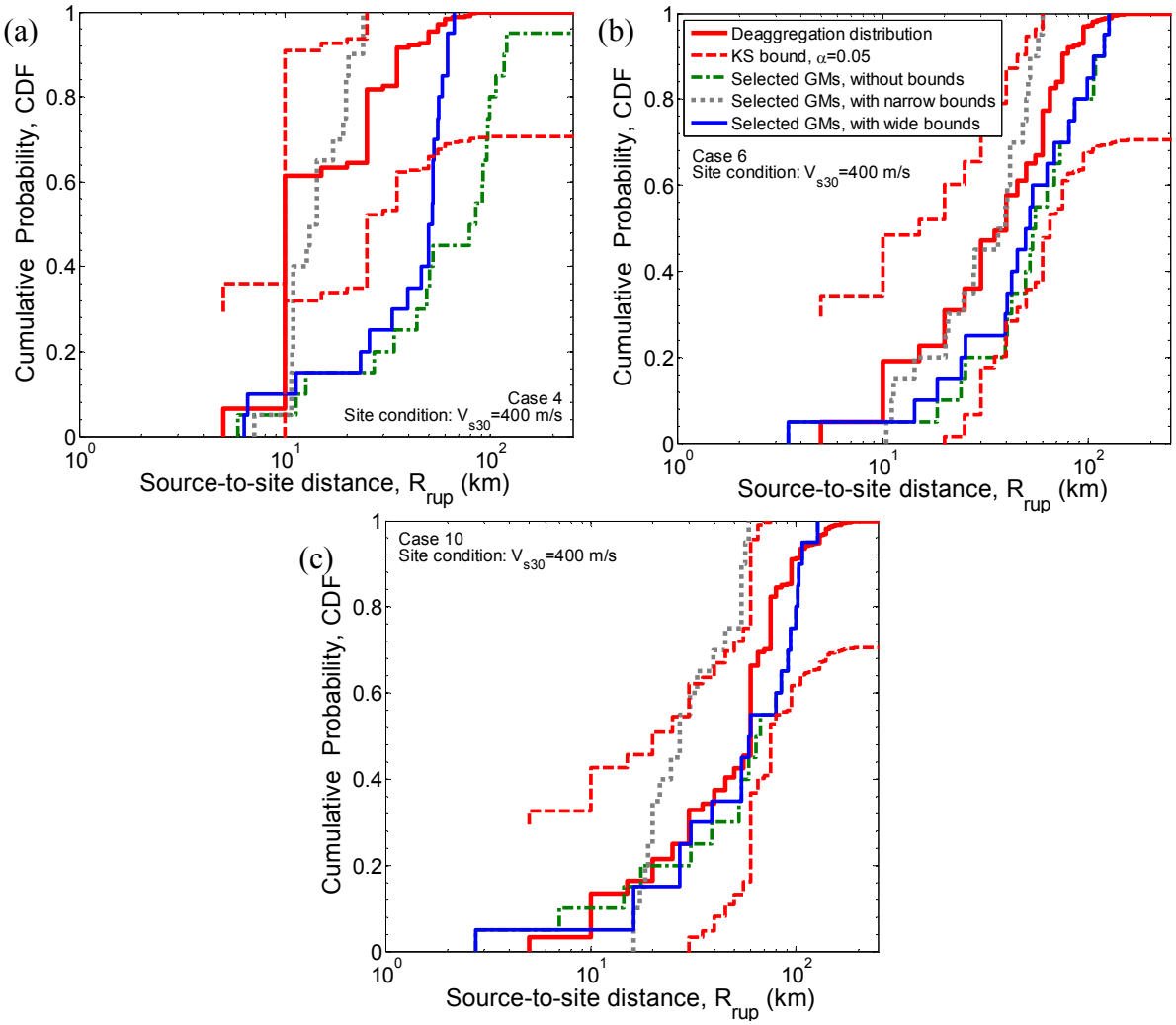

Figure 25: Comparison between source-to-site distance distribution of selected ground motions and the deaggregation results for sample PSHA cases with V_{s30}=400 m/s site condition: (a) case 4; (b) case 6; (c) case 10.

In order to compare the site condition distribution of selected ground motions with the corresponding target site condition, Figure 26 presents the V_{s30} distribution of selected ground motions for a sample PSHA case with V_{s30}=200, 400, and 800 m/s site conditions. It

is noted that using wide or narrow bounds only affects the number of available ground motions through the applied bounds on M_w and R_{rup}, as the V_{s30} bound is the same for both narrow and wide bounds. Also, since the PSHA case used in Figure 26 is the same across the presented results, the M_w and R_{rup} bounds applied on the prospective ground motions are constant. Thus, only the V_{s30} bound has the main effect on the V_{s30} distribution of selected ground motions presented in Figure 26.

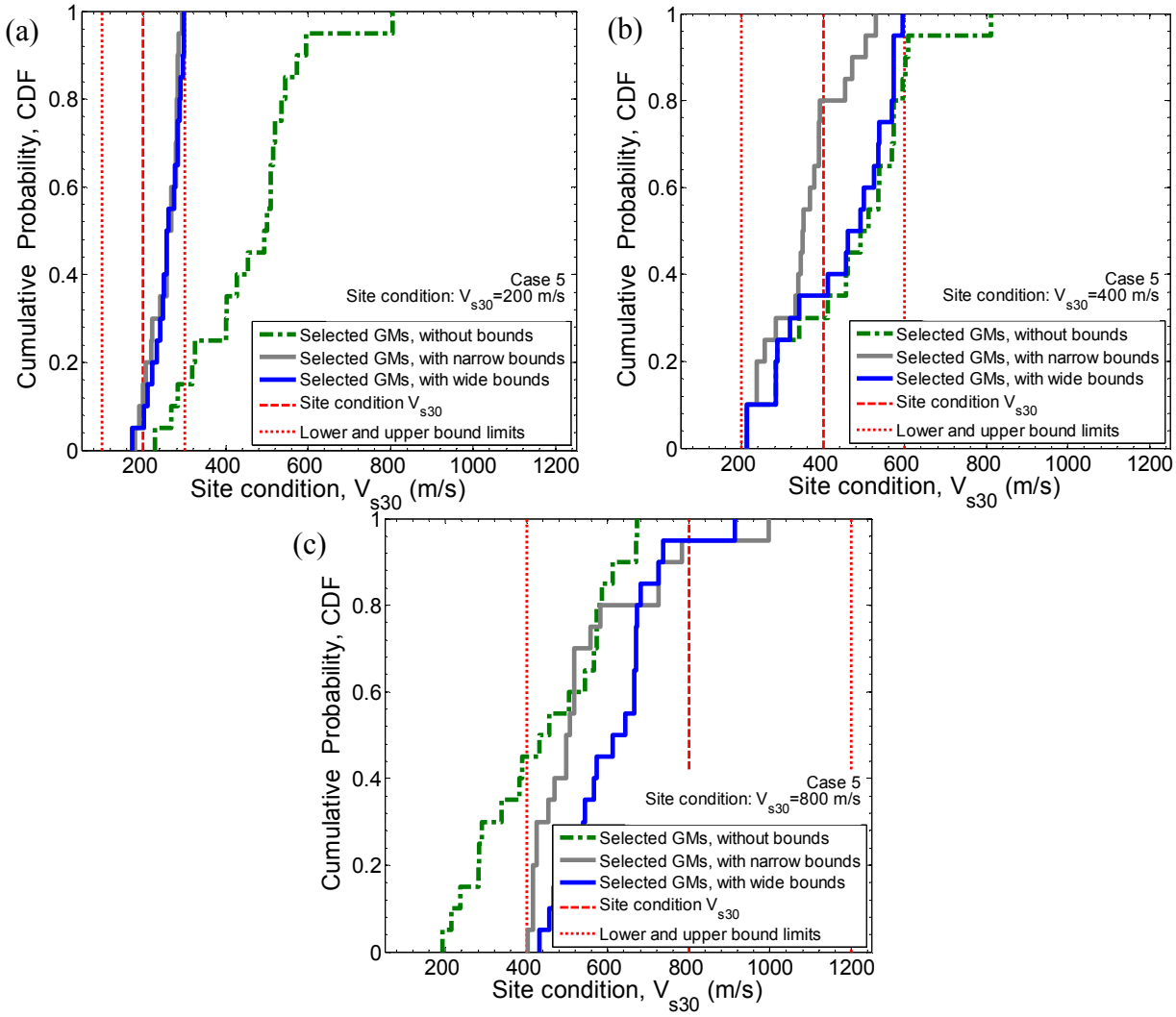

Figure 26: Comparison between V_{s30} distribution of selected ground motions and the target V_{s30} for a sample PSHA case representing three site conditions considered: (a) V_{s30}=200 m/s; (b) V_{s30}=400 m/s; (c) V_{s30}=800 m/s.

As shown in Figure 26a, the V_{s30} values of selected ground motions with or without bounds for soft soil condition (i.e., V_{s30}=200 m/s) are generally greater than the target V_{s30} value. This is caused by a paucity of available ground motions in the database recorded on soft soil sites, as previously illustrated in Table 13. As presented in Figure 26a, selecting ground motions without bounds results in motions with V_{s30} values up to 800 m/s to represent

the target V_{s30}=200 m/s site condition, whereas, ground motions selected based on bounds (narrow or wide) results in motions within the specified bounds (i.e., $100 \leq V_{s30} \leq 300$ m/s), representing the soft soil condition.

As shown in Figure 26b for the stiff soil condition (i.e., V_{s30}=400 m/s), selected ground motions without bounds and with wide bounds have an appropriate representation of the target site condition with the median V_{s30} close to the target value. In some PSHA cases with stiff soil condition such as case 5 presented in Figure 26b, ground motions selected based on narrow bounds have a weaker representation (either large or smaller median value) in comparison to the ground motions selected based on wide bounds and without bounds. This is caused by removing an excessive number of ground motion through the narrow M_w and R_{rup} bounds.

As shown in Figure 26c for soft rock condition (i.e., V_{s30}=800 m/s), half of the ground motions selected without bounds have V_{s30} values smaller than 400 m/s for the considered PSHA case, whereas, half of the ground motions selected based on wide bounds have V_{s30} values greater than 600 m/s, indicating an improved representation of the target site condition for ground motions selected based on wide bounds in comparison to those selected based on no bounds. The V_{s30} distribution of ground motions selected based on narrow bounds is similar to those selected based on wide bounds.

In order to investigate the effect of causal parameter bounds on amplitude scaling factors of selected ground motions, Figure 27 presents the distribution of scaling factors of ground motions selected for the same sample PSHA case presented in Figure 26 with V_{s30}=200, 400, and 800 m/s site conditions. As shown in Figure 27a-c, ground motions selected based on the narrow bounds have lower scaling factors compared to those selected based on no bounds or wide bounds for all three site conditions considered. As already mentioned for scenario-based ground motion selection (section 2.4.2), this is due to the fact that by restricting the prospective ground motions to those motions with causal parameters close to characteristics of the causal ruptures affecting the seismic hazard, only a small change in amplitude of as-recorded motions is required to represent the target distribution of IMs. It is important to note that having small amplitude scaling factors does not imply a higher quality in terms of representing the target distribution (both mean and variability) of the considered explicit IMs. This issue is illustrated in Figure 18 to Figure 23, as ground

motions selected based on narrow bounds have a poor representation of the target IM distributions.

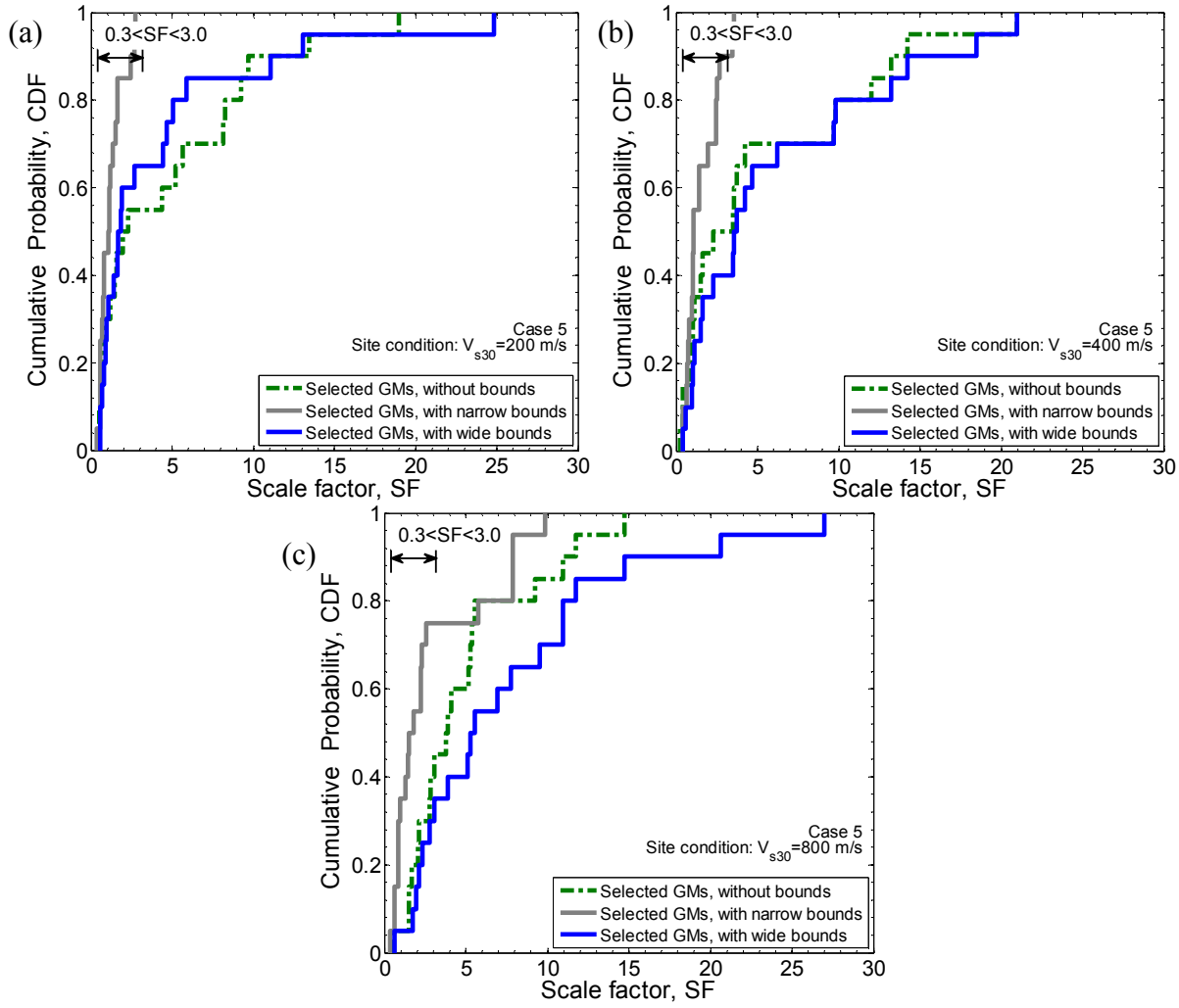

Figure 27: Amplitude scaling factor distribution of selected ground motions for a sample PSHA case representing the three site conditions: (a) V_{s30}=200 m/s; (b) V_{s30}=400 m/s; (c) V_{s30}=800 m/s.

As shown in Figure 27a as an example for PSHA cases with V_{s30}=200 m/s site condition, ground motions selected based on wide bounds have mostly lower scaling factors compared to those selected based on no bounds. As presented in Figure 27b as an example for PSHA cases with V_{s30}=400 m/s site condition, the applied scaling factors on ground motions selected based on wide bounds are similar to those selected based on no bounds. This holds true for PSHA cases with V_{s30}=800 m/s site condition as well, except for some cases such as that presented in Figure 27c, in which ground motion selected based on wide bounds have larger scaling factors compared to those selected based on no bounds.

3.4 The effect of causal parameter bounds on the computational efficiency of PSHA-based ground motion selection

Similar to the scenario-based ground motion selection, considering bounds on the causal parameters reduces the size of prospective ground motion database and consequently this can reduce the computational time for PSHA-based ground motion selection. Figure 28 compares the computational cost of conducting ground motion selections without bounds and with wide bounds for all of the considered PSHA cases with V_{s30}=200, 400, and 800 m/s site conditions. Similar to the scenario cases, the computational cost is measured based on the time spent to select an ensemble of 20 ground motions by conducting 10 replicate selections using a typical desktop computer (i.e., a Pentium 4 processor with 2.93 GHz CPU and 4GB RAM).

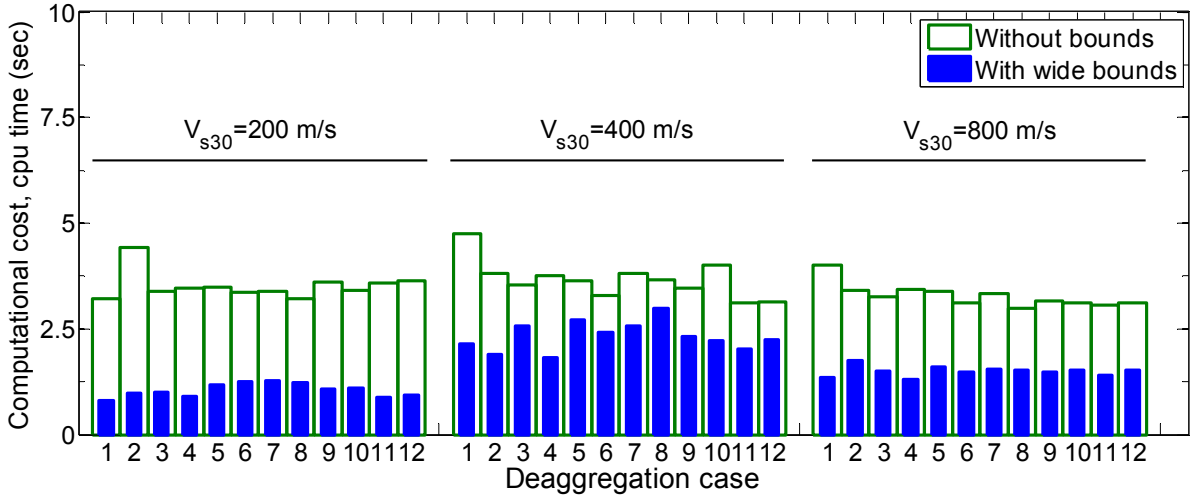

Figure 28: Comparison between the computational cost of ground motion selection without bounds and with wide bounds for the considered PSHA cases with V_{s30}=200, 400, and 800 m/s site conditions

As shown in Figure 28, bound consideration lowers the computational time of ground motion selection for all of the PSHA cases considered. However, it is noted that the computational time for PSHA-based ground motion selection is significantly lower in comparison to the scenario-based ground motion selection (i.e., in the order of few seconds as compared to tens of minutes). This is due to the fact that the amplitude scaling factors of prospective ground motions in the PSHA-based ground motion selection is easily obtained from an algebraic equation (Bradley 2012c, equation (13)), whereas for scenario-based ground motion selection optimization is required to obtained the scaling factors (Tarbali and Bradley 2014b, equation (5)). Based on the obtained results in Figure 28, it can be seen that the computational cost of PSHA-based ground motion selection can be negligible whether

causal parameter bounds are considered or not. Nevertheless, application of the causal parameter bounds can assist in reducing the size of the prospective ground motion database, especially if the number of ground motions outside of the considered bounds is large.

4 Conclusion

Using bounds on the causal parameters of prospective ground motions (e.g., magnitude, source-to-site distance, and site condition) is common practice in conventional approaches for ground motion selection. The primary reason for using causal parameter bounds stems from the fact that considering spectral acceleration (SA) ordinates as the only explicit intensity measure does not account for an accurate representation of ground motion duration and cumulative effects which are not explicitly considered. Despite the prevalent application of causal parameter bounds, there is no consistent approach for setting bounds as a function of the seismic hazard at the site. In this study, the effect of using bounds on causal parameters of prospective ground motions for the purpose of ground-motion selection for scenario and probabilistic seismic hazard analysis (PSHA) is investigated. 78 scenario and 36 PSHA cases were considered for ground motion selection with and without the application of causal parameter bounds, which cover a wide range of seismic scenarios and site conditions. Ground motions were selected based on the generalized conditional intensity measure (GCIM) approach, which considers multiple ground motion intensity measures (IMs) and their variability in order to appropriately represent characteristics of the seismic hazard at the site.

The inadequacy of using bounds to account for shortcomings of selecting ground motions based on only SA ordinates was firstly illustrated by performing ground motion selection for the considered scenario and PSHA cases with and without the consideration of causal parameter bounds, in which the distributions of non-SA IMs were seen to be inconsistent between the selected ground motions and the target distributions for the seismic hazard considered.

By considering different aspects of ground motion severity, including amplitude, frequency content, duration, and cumulative effects through the GCIM-based ground motion selection, the effects of causal parameter bounds on characteristics of the selected ground motions were investigated. It was demonstrated that the application of relatively ‘wide’ bounds on causal parameters can effectively remove ground motions with drastically different characteristics than the target seismic hazard, leading to an improvement in the computational efficiency of the selection process by reducing the subset of prospective

records, especially for scenario-based ground motion selections relative to PSHA-based selections. In addition to an improvement in computational efficiency of the ground motion selection process, application of wide bounds improves the representation of causal parameters of the selected ground motions to the target seismic hazard characteristics, and does not degrade the quality of the selected ground motions to represent the target distribution of explicit IMs (which is the primary aim in the ground motion selection process). In contrast, the use of excessively narrow bounds can lead to ground motion ensembles with a poor representation of the target IM distributions, as a result of the narrow bounds resulting in a small database of prospective ground motions relative to the size of the ground motion ensemble desired. It was heuristically evaluated that the subset of prospective ground motions after the application of causal parameter bounds should be a factor of three or more greater than the ground motion ensemble size desired.

The specific causal parameter bound criteria advocated in this study (i.e., criterion AC) is recommended for general use in ground motion selection from PSHA results as a 'default' bounding criterion. However, if such a criterion results in an excessively small subset of prospective ground motions then variations from this default should be considered.

References

Ancheta, T. D., Darragh, R., Stewart, J., Seyhan, E., Silva, W., Chiou, B., Wooddell, K., Graves, R., Kottke, A. and Boore, D. (2013). "PEER NGA-West2 Database." *PEER Report 2013* **3**.

ASCE/SEI7-10 (2010). Minimum Design Loads for Buildings and Other Structures, ASCE/SEI 7-10. American Society of Civil Engineers, Reston, Virginia.

Baker, J. W. (2010). "Conditional mean spectrum: Tool for ground-motion selection." *Journal of Structural Engineering* **137**(3): 322-331.

Baker, J. W. and Cornell, A. C. (2006). "Spectral shape, epsilon and record selection." *Earthquake Engineering & Structural Dynamics* **35**(9): 1077-1095.

Baker, J. W. and Jayaram, N. (2008). "Correlation of spectral acceleration values from NGA ground motion models." *Earthquake Spectra* **24**(1): 299-317.

Bommer, J. J. and Acevedo, A. B. (2004). "The use of real earthquake accelerograms as input to dynamic analysis." *Journal of Earthquake Engineering* **8**(spec01): 43-91.

Bommer, J. J., Douglas, J. and Strasser, F. O. (2003). "Style-of-faulting in ground-motion prediction equations." *Bulletin of Earthquake Engineering* **1**(2): 171-203.

Bommer, J. J., Magenes, G., Hancock, J. and Penazzo, P. (2004). "The influence of strong-motion duration on the seismic response of masonry structures." *Bulletin of Earthquake Engineering* **2**(1): 1-26.

Bommer, J. J., Stafford, P. J. and Alarcón, J. E. (2009). "Empirical equations for the prediction of the significant, bracketed, and uniform duration of earthquake ground motion." *Bulletin of the Seismological Society of America* **99**(6): 3217-3233.

Boore, D. M. and Atkinson, G. M. (2008). "Ground-motion prediction equations for the average horizontal component of PGA, PGV, and 5%-damped PSA at spectral periods between 0.01 s and 10.0 s." *Earthquake Spectra* **24**(1): 99-138.

Bozorgnia, Y., Abrahamson, N. A., Atik, L. A., Ancheta, T. D., Atkinson, G. M., Baker, J. W., Baltay, A., Boore, D. M., Campbell, K. W. and Chiou, B. S.-J. (2014). "NGA-West2 research project." *Earthquake Spectra*.

Bradley, B. A. (2010a). "A generalized conditional intensity measure approach and holistic ground-motion selection." *Earthquake Engineering & Structural Dynamics* **39**(12): 1321-1342.

Bradley, B. A. (2010b). "Site-Specific and Spatially Distributed Ground-Motion Prediction of Acceleration Spectrum Intensity." *Bulletin of the Seismological Society of America* **100**(2): 792-801.

Bradley, B. A. (2011a). "Correlation of significant duration with amplitude and cumulative intensity measures and its use in ground motion selection." *Journal of Earthquake Engineering* **15**(6): 809-832.

Bradley, B. A. (2011b). "Empirical correlation of PGA, spectral accelerations and spectrum intensities from active shallow crustal earthquakes." *Earthquake Engineering & Structural Dynamics* **40**(15): 1707-1721.

Bradley, B. A. (2011c). "Empirical equations for the prediction of displacement spectrum intensity and its correlation with other intensity measures." *Soil Dynamics and Earthquake Engineering* **31**(8): 1182-1191.

Bradley, B. A. (2012a). "Empirical correlations between cumulative absolute velocity and amplitude-based ground motion intensity measures." *Earthquake Spectra* **28**(1): 37-54.

Bradley, B. A. (2012b). "Empirical correlations between peak ground velocity and spectrum-based intensity measures." *Earthquake Spectra* **28**(1): 17-35.

Bradley, B. A. (2012c). "A ground motion selection algorithm based on the generalized conditional intensity measure approach." *Soil Dynamics and Earthquake Engineering* **40**: 48-61.

Bradley, B. A. (2013). Ground motion selection for seismic risk analysis of civil infrastructures. Handbook of seismic risk analysis and management of civil infrastructure systems. S. Tasfamariam and K. Goda. Cambridge, Woodhead Publishing Ltd.

Bradley, B. A., Cubrinovski, M., MacRae, G. A. and Dhakal, R. P. (2009). "Ground-motion prediction equation for SI based on spectral acceleration equations." *Bulletin of the Seismological Society of America* **99**(1): 277-285.

Campbell, K. W. and Bozorgnia, Y. (2010). "A ground motion prediction equation for the horizontal component of cumulative absolute velocity (CAV) based on the PEER-NGA strong motion database." *Earthquake Spectra* **26**(3): 635-650.

CEN (2005). Design of Structures for Earthquake Resistance. Part 1: General Rules, Seismic Actions and Rules for Buildings.

Chiou, B., Darragh, R., Gregor, N. and Silva, W. (2008). "NGA project strong-motion database." *Earthquake Spectra* **24**(1): 23-44.

Field, E. H., Jordan, T. H. and Cornell, C. A. (2003). "OpenSHA: A developing community-modeling environment for seismic hazard analysis." *Seismological Research Letters* **74**(4): 406-419.

Jayaram, N., Lin, T. and Baker, J. W. (2011). "A computationally efficient ground-motion selection algorithm for matching a target response spectrum mean and variance." *Earthquake Spectra* **27**(3): 797-815.

Katsanos, E. I., Sextos, A. G. and Manolis, G. D. (2010). "Selection of earthquake ground motion records: A state-of-the-art review from a structural engineering perspective." *Soil Dynamics and Earthquake Engineering* **30**(4): 157-169.

Kottke, A. and Rathje, E. M. (2008). "A semi-automated procedure for selecting and scaling recorded earthquake motions for dynamic analysis." *Earthquake Spectra* **24**(4): 911-932.

McGuire, R. K. (1995). "Probabilistic seismic hazard analysis and design earthquakes: closing the loop." *Bulletin of the Seismological Society of America* **85**(5): 1275-1284.

NEHRP (2003). Building Seismic Safety Council, NEHRP Recommended Provisions for seismic Regulations for New buildings and other Structures, Part1: Provisions, FEMA 368, Federal Emergency Management Agency, Washington, D.C.

NZS1170.5 (2004). NZS1170.5:2004 Structural design actions, Part 5: Earthquake actions - New Zealand. Wellington, NZ, Standards New Zealand.

Petersen, M. D., Cao, T., Campbell, K. W. and Frankel, A. D. (2007). "Time-independent and time-dependent seismic hazard assessment for the State of California: Uniform California Earthquake Rupture Forecast Model 1.0." *Seismological Research Letters* **78**(1): 99-109.

Shome, N., Cornell, C. A., Bazzurro, P. and Carballo, J. E. (1998). "Earthquakes, records, and nonlinear responses." *Earthquake Spectra* **14**(3): 469-500.

Stewart, J. P., Chiou, S.-J., Bray, J. D., Graves, R. W., Somerville, P. G. and Abrahamson, N. A. (2001). Ground motion evaluation procedures for performance-based design. PEER report 2001/09, Pacific Earthquake Engineering Research Center, University of California, Berkeley.

Tarbali, K. and Bradley, B. A. (2014a). Ground-motion selection for scenario ruptures using the generalized conditional intensity measure (GCIM) approach and its application for several major earthquake scenarios in New Zealand. Department of Civil and Natural Resources Engineering, University of Canterbury, New Zealand, https://sites.google.com/site/brendonabradley/publications**:** 92.

Tarbali, K. and Bradley, B. A. (2014b). "Ground-motion selection for scenario ruptures using the generalized conditional intensity measure (GCIM) method." *Earthquake Engineering & Structural Dynamics* **(In-press)**.

Wang, G. (2011). "A ground motion selection and modification method capturing response spectrum characteristics and variability of scenario earthquakes." *Soil Dynamics and Earthquake Engineering* **31**(4): 611-625.

Wang, G., Youngs, R., Power, M. and Li, Z. (2013). "Design Ground Motion Library (DGML): An Interactive Tool for Selecting Earthquake Ground Motions." *Earthquake Spectra* **(In-press)**.